

Interaction of the lithospheric mantle and crustal melts for the generation of the Horoz pluton (Niğde, Turkey): whole-rock geochemical and Sr–Nd–Pb isotopic evidence

Kerim Kocak^a and Veysel Zedef^b

^a Department of Geological Engineering, Selcuk University, Campus, 42075 Konya, Turkey; kkokak@yahoo.com

^b Department of Mining Engineering, Selcuk University, 42070 Konya, Turkey

Received 31 March 2016, accepted 7 July 2016

Abstract. The Horoz pluton includes granitic and granodioritic rocks, with widespread mafic microgranular enclaves (MMEs). Petrochemically, the rocks of the pluton show calc-alkaline to shoshonitic and metaluminous to slightly peraluminous composition. The rocks also exhibit an enrichment in large ion lithophile elements, e.g. Rb, K, and depletions of high field strength elements such as Y, Lu, and Mg#, Ni, with a slightly concave-upward rare earth element pattern. Both granitic and granodioritic rocks exhibit geochemical characteristics of tonalite, trondhjemite and granodiorite assemblages, possibly developed by the partial melting of a thickened lower crust. The granitoids have high concentrations of Na₂O (2.6–4.5 wt%), Sr (347–599 ppm), intermediate-high (La/Yb)_N (8.2–18.1, mostly >11), Al₂O₃ (13.2–16.9 wt%, average 15.3 wt%), low MgO (0.2–1.4 wt%, average 0.84 wt%) and Co (0.7–10.3 ppm). The MMEs include higher Na₂O (4.5–5.5 wt%), Sr (389–1149 ppm), Al₂O₃ (16.9–19.2 wt%, average 17.8 wt%), MgO (1.4–4.4 wt%, average 2.75 wt%) and Co (6.2–18.7 ppm) contents in comparison with that of their hosts. There is a lack of negative Eu anomalies, except a few samples. Both host rocks and MMEs have a low initial ⁸⁷Sr/⁸⁶Sr ratio (respectively 0.7046–0.7051 and 0.7047–0.7058), low ε_{Nd} value (–1.8 to –0.2 and –0.6 to 0.7 at 50 Ma) and highly radiogenic ²⁰⁸Pb/²⁰⁴Pb ratios (39.43–39.47 and 39.39–39.54).

Whole-rock chemistry and isotopic data suggest that parent magmas of both MMEs and their hosts have derived from melts of the mixing between the lithospheric mantle and crustal end members, than fractional crystallization processes in crustal levels.

Key words: granite, mafic microgranular enclave, magma mixing, Sr–Nd–Pb isotopes, TTG, Turkey.

INTRODUCTION

Mafic microgranular enclaves (MMEs) are common in metaluminous to peraluminous granitoid plutons (Cantagrel et al. 1984; Bacon 1986; Didier & Barbarin 1991), and are also abundant in most of the Alpine granitoids of Turkey (e.g. Kocak 1993, 2006, 2008; Çevikbaş et al. 1995; Kadioglu & Güleç 1996; Arslan & Aslan 2006; Aydoğan et al. 2008; Kaygusuz & Aydınçakır 2009; Kocak et al. 2011). They contain mafic mineral assemblages, are relatively fine-grained and have general ellipsoidal shape with unique microstructures commonly interpreted as being igneous as reported in many petrological papers (e.g. Didier 1973; Vernon 1984, 1990; Frost & Mahood 1987; Bédard 1990; Dodge & Kistler 1990; Srogi & Lutz 1990; Poli & Tommasini 1991; Barbarin & Didier 1992; Silva et al. 2000; Waight et al. 2001; Barbarin 2005).

Mafic microgranular enclaves provide significant information on the nature of source rocks, the genesis of granitic magma (Pin et al. 1990; Didier & Barbarin 1991; Barbarin & Didier 1992; Anderson et al. 1998;

Waight et al. 2001), the coexistence of two contrasting magma types (Dorais et al. 1990; Vernon 1990), the rheology of host magmas and the tectonic environments of granitoid rocks, as well as on the interaction between the continental crust and the mantle (Didier et al. 1982). Therefore, their origin is of essential significance in interpreting the history of plutons. The Horoz pluton (HP) is a typical example of bimodal magmatism on the northern margin of the Tauride belt. We present detailed whole-rock chemical and Sr–Nd–Pb isotopic data of the MMEs and host granitoids from the HP, and use these data to constrain in granitic plutonism.

GEOLOGICAL SETTING

Turkey is an essential east–west trending constituent of the Alpine–Himalayan orogenic system and contains several continental and oceanic fragments assembled due to the closure of different Tethyan oceanic basins during the Late Cretaceous–Early Tertiary period (Fig. 1a). One of these basins in southern Turkey, namely the

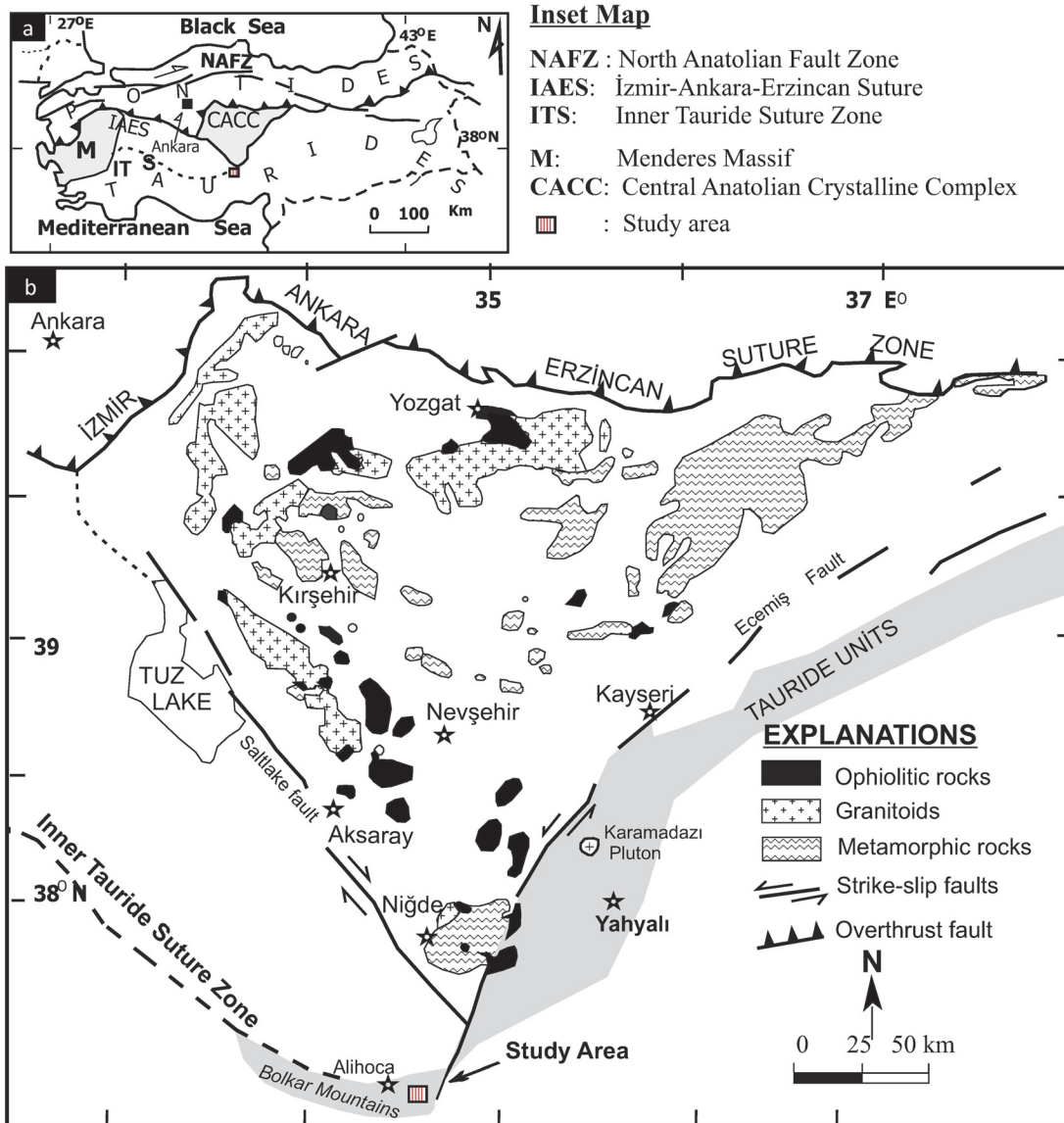


Fig. 1. Generalized geological sketch map of the main lithologic units of the Central Anatolian Crystalline Complex (after Bingöl 1974).

Inner Tauride Ocean (Gorur et al. 1984; Dilek et al. 1999; Ozer et al. 2004), was formed between the Central Anatolian Crystalline Complex (CACC) and the Tauride carbonate platform. The CACC is the largest metamorphic block exposed in Turkey and consists of Upper Palaeozoic (Kocak 1993; Kocak & Leake 1994) interlayered metacarbonate and metapelitic rocks. The ocean was then consumed as a result of north-dipping subduction and closed during the latest Cretaceous to early Cenozoic times (Parlak et al. 2013a), as evidenced by the existence of discontinuous exposures of the Cenomanian–Turonian suprasubduction zone ophiolites (i.e. Alihoca, Aladag) and mélanges by latest Cretaceous time (Clark &

Robertson 2002) along the Inner-Tauride Suture Zone (Fig. 1a, b). Though the ophiolitic exposures along the suture zone are covered by the Ulukisla Basin strata, the existence of high positive magnetic anomalies corresponding to the Inner-Tauride Suture Zone (Kaynak & Akçakaya 2006) also supports the development of the Inner Tauride Ocean and associated oceanic lithosphere through the late Mesozoic and thus the derivation of the Tauride ophiolites from this oceanic root. The collision of Tauride and CACC continental blocks during the Palaeocene led to the southward transport of the already-emplaced ophiolites and mélanges and flysch formation together with folding.

The NE–SW trending HP is situated in the eastern part of the Bolkar Mountains as a part of the Tauride Platform (Fig. 1b). The pluton formed nearby the Inner-Tauride Suture Zone and intruded into the Bolkar Mountain units, which include variably metamorphosed, Upper Permian–Upper Triassic platform carbonates with siliciclastic intercalations. The HP contains granite and granodiorite members (Fig. 2) and has sharp and discordant contacts, with hornfels formation, which suggests a shallow-crustal emplacement depth. The HP is intruded by two types of mafic dykes with sharp contacts: (i) the blackish-coloured dyke closely associated with granitoids and dismembered in places, forming smaller angular enclaves and (ii) the greenish-coloured dyke forming relatively alteration-resistant, higher topographic levels in the northwestern part of the study area. It contains also some small felsic enclaves and has sharp contacts with their granitoid host rocks, representing possibly the youngest magmatic unit in the pluton. The HP was intruded into the Upper Cretaceous Alihoca ophiolites, which include ultrabasic rocks, volcanosedimentary rocks, volcanic rocks, diabases, spilite and glaucophane-bearing schists. In comparison with the felsic granite, the granodiorite is relatively coarse-grained,

less fractured/altered and has more enclaves. Based on the existence of pebbles of the Horoz granitoid (Alan et al. 2007) in the Middle Eocene clastic rocks of the Ulukisla–Çamardı basin, the age of the Horoz granitoid is constrained as the Palaeocene–early Eocene. Geochronological studies suggest a crystallization age between 49 and 56 Ma by U–Pb zircon dating (Kadioglu & Dilek 2010; Kuscu et al. 2010; Parlak et al. 2013b) and ^{40}Ar – ^{39}Ar dating (Kuscu et al. 2010). The HP was unroofed due to crustal uplift and erosion throughout the Palaeogene by 23.6 ± 1.2 Ma (Dilek et al. 1997). However, a recent study (Whitney et al. 2015) suggests that the Horoz granitoid records two main pulses of cooling: (1) an initial stage at ~ 38 – 31 Ma, possibly linked with a regional event that is recorded in other crystalline rocks in Central Anatolia and (2) a later stage that may correspond to at least ~ 2 km of erosion-related exhumation associated with late Miocene uplift of the southern margin of the Central Anatolian Plateau.

Rounded MMEs in the pluton have usually fine-grained margins and different sizes, from several centimetres up to metres. The geometry of the enclave–host contact varies from sharp/crenulate to diffuse/veined. The contact also varies from lobate to cusped (Fig. 3a, b).

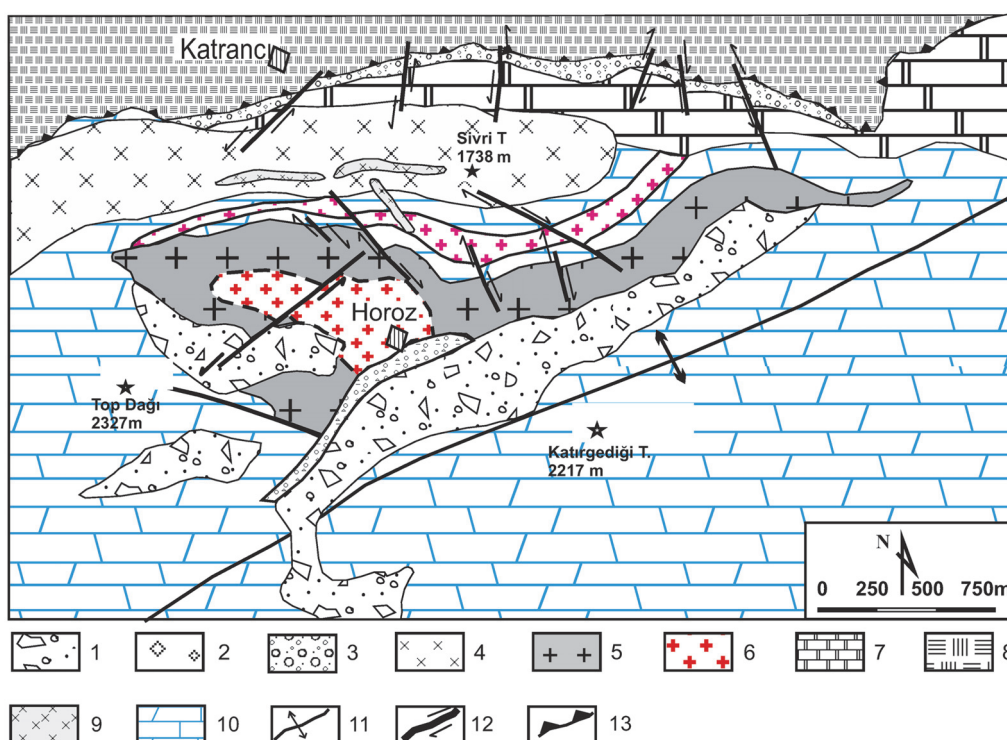


Fig. 2. Geological map of the Horoz area (modified from Çevikbaş et al. 1995 and Kadioglu & Dilek 2010). 1, Talus (Quaternary); 2, terrace (Plio-Quaternary); 3, Geyikpınarı conglomerate member (Palaeocene); 4, Yataктаş quartz-porphphyry (U. Cretaceous–Palaeocene); 5, granite (Eocene); 6, granodiorite (Eocene); 7, Kalkankaya formation (U. Maestrichtian–L. Palaeocene); 8, Alihoca ophiolitic complex (Cretaceous); 9, Madenköy ophiolitic mélangé (Cretaceous); 10, Bolkardağı marble (Permian); 11, anticline; 12, wrench fault; 13, thrust fault.

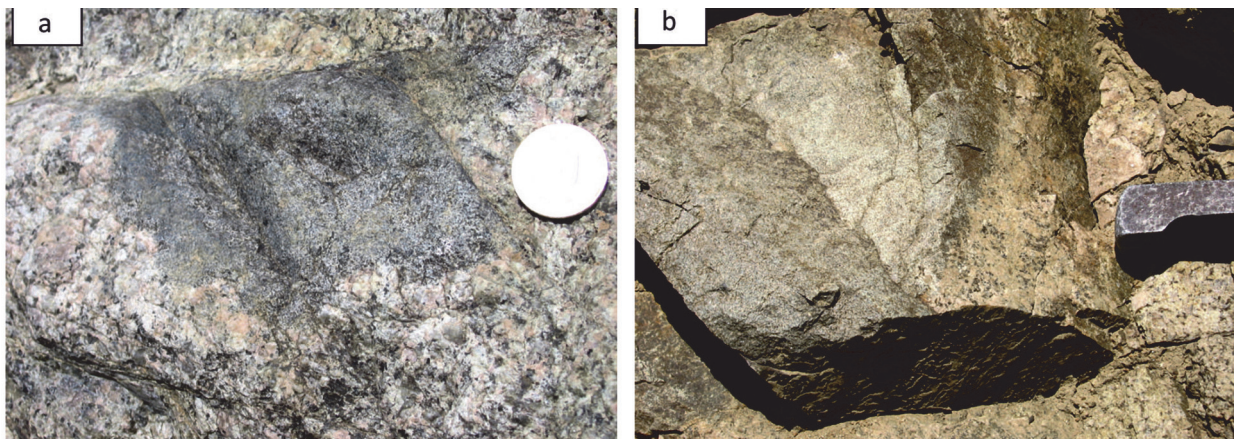


Fig. 3. Field photographs of MMEs displaying sharp (a) and cusped (b) contacts with granodiorite (a) and granite (b).

The MMEs in the dioritic dykes may include a ‘double enclave’ structure where they partially or fully contain smaller, finer-grained, more mafic enclaves. The MMEs sometimes show core-tail structures, in which the tail displays an S-shaped bend, suggesting that they were at least partly plastic when introduced into the felsic magma.

PETROGRAPHY

The host rocks and their enclaves are usually equigranular and holocrystalline, but porphyritic texture also exists in the enclaves. The main constituents in the granitoids are plagioclase (An_{17-55}), quartz, biotite (mostly eastonitic), orthoclase and amphibole (magnesian hornblende and edenite), with accessory acicular apatite and zircon in a hipidiomorphic granular texture (Kocak et al. 2011). The MMEs have similar mineralogy with their host. Major components are plagioclase (An_{18-64} , 75–85%), amphibole (5–15%), biotite (5–10%), orthoclase (0–5%) and minor quartz, titanite and acicular and stubby prismatic apatite. The texture is mostly equigranular and fine-grained, but sometimes porphyritic and poikilitic. The greenish dyke is predominantly made up of plagioclase, hornblende, chlorite and minor quartz in a holocrystalline porphyritic texture.

ANALYTICAL METHODS

Whole-rock major and trace element analyses of 29 samples were performed at Acme Lab. Ltd. (Vancouver, Canada). Major oxide and trace element compositions were determined by the inductively coupled plasma emission spectrometer from pulps after 0.2 g rock powder was fused with 1.5 g $LiBO_2$ and then dissolved

in 100 mm³ 5% HNO_3 . Rare earth elements (REEs) were analysed by inductively coupled plasma mass spectrometry from pulps after 0.25 g rock powder was dissolved with four acid digestions. Analytical uncertainties vary from 0.1% to 0.04% for major elements, from 0.1% to 0.5% for trace elements and from 0.01 to 0.5 ppm for REEs.

Sr, Nd and Pb isotope compositions were determined using a Finnigan Mat 262 mass spectrometer at the GEOMAR research centre (Kiel, Germany). Replicate analyses of Sr–Nd–Pb isotopes on the same samples at GEOMAR were within the analytical uncertainties. Sr was measured in static mode and $^{87}Sr/^{86}Sr$ normalized within-run to $^{86}Sr/^{88}Sr = 0.1194$. NBS 987 gave an $^{87}Sr/^{86}Sr$ ratio of 0.710240 ± 0.000008 . The acid washed samples were boiled in 6N HCL for 1 h. The $^{143}Nd/^{144}Nd$ ratio was normalized within-run to $^{146}Nd/^{144}Nd = 0.7219$ and measured in static mode where the Nd standard La Jolla yielded an average ratio of $^{143}Nd/^{144}Nd = 0.51196276$. All Pb isotope analyses were corrected to NBS 981 (Todd et al. 1996) for fractionation. Sample reproducibility is estimated at ± 0.02 , ± 0.015 and ± 0.03 (2σ) for $^{206}Pb/^{204}Pb$, $^{207}Pb/^{204}Pb$ and $^{208}Pb/^{204}Pb$ ratios, respectively.

RESULTS

Whole-rock geochemistry

The whole-rock chemical compositions of representative samples from HP host rocks and their MMEs are listed in Table 1.

The granitic rock samples of the HP plot mostly in the granite, monzogranite (adamellite) and granodiorite fields with minor tonalite, whereas samples of MMEs primarily plot in the fields of quartz monzodiorite/monzogabbro, quartz diorite/gabbro (Fig. 4a) with

Table 1. Major (wt%), trace and rare-earth element (ppm) analyses of the Horoz pluton

Sample	Enclave											Dyke	
	12	15	23	h36	11b	13a	17b	18a	21a	24a	40a	42	43
SiO ₂	56	55.8	56	58.9	57.9	58.5	59.3	62.8	57.3	58.7	57	55.3	56.8
TiO ₂	0.72	0.65	0.75	0.37	0.6	0.61	0.48	0.4	0.63	0.58	0.58	0.71	0.69
Al ₂ O ₃	17.3	18.7	16.9	19.2	18.2	17.7	17.3	17.5	18.1	17	18.3	17.6	17.4
Fe ₂ O ₃ t	8.09	6.95	7.06	5.58	6.61	7.26	7.38	4.5	6.33	5.43	5.79	5.74	6.96
MgO	3.28	3.25	4.37	1.47	2.66	2.25	2.38	1.43	3.17	3.44	2.51	3.93	4.47
MnO	0.18	0.19	0.28	0.1	0.16	0.14	0.14	0.09	0.19	0.22	0.17	0.08	0.08
CaO	5.05	4.86	5.89	4.5	4.92	4.1	3.54	3.84	5.73	5.25	5.43	5.64	5.36
Na ₂ O	5.04	4.98	4.57	4.81	5.49	4.68	4.59	4.48	5.3	4.97	4.71	4.22	4.14
K ₂ O	1.2	1.5	0.92	2.65	0.98	2.77	3.12	3.18	1.03	1.92	2.3	1.89	1.67
P ₂ O ₅	0.42	0.25	0.19	0.38	0.25	0.22	0.2	0.27	0.19	0.2	0.23	0.25	0.23
LOI	2.5	2.9	3	1.9	2.1	1.7	1.5	1.5	1.9	2.3	2.9	4.4	2
Total	99.8	100	99.9	99.9	99.9	99.9	100	100	99.9	100	99.9	95.4	99.8
Ni	3.7	4.5	14.1	3.2	5.7	4.4	8.2	2.5	5.5	5.3	5.5	53	47.3
Cr	bdl	20	100	bdl	20	20	30	bdl	10	40	bdl	200	190
Co	11	11	19	6	18	7	8	6	14	11	12	18	19
Ga	21	23	20	19	20	20	19	18	18	18	19	17	16
Rb	46	40	40	72	35	63	75	68	47	57	85	57	56
Sr	1149	509	389	807	436	456	481	592	551	433	549	909	892
Ba	222	267	157	373	163	317	411	376	176	209	420	629	458
Zr	124	142	97	120	143	119	144	197	113	101	133	140	141
Nb	24	31	32	30	30	37	28	21	14	22	34	11	11
Ta	2	2	2	3	2	3	2	2	1	1	2	1	1
Th	15	7	9	6	10	11	13	14	7	10	9	7	7
U	5	11	4	3	4	5	5	5	3	6	7	2	2
Y	50	44	44	76	42	51	41	30	23	31	49	22	21
La	79.2	13.1	18.4	15.4	17.2	16.6	17.9	14.3	14.3	21.2	12.5	30.6	26.3
Ce	174	36.9	52.4	44.9	51.6	55.4	50.5	37.6	35.4	58.4	38.7	61.3	55.9
Pr	20.2	5.22	6.87	6.81	7.07	7.79	6.78	4.79	4.12	7.36	5.85	6.64	6.3
Nd	74.7	22	26	33.3	27.6	33	27.1	19.2	16.5	28.4	25.8	24.1	23.8
Sm	11.1	5.04	5.18	9.36	5.79	6.8	5.85	3.82	3.06	5.2	6.51	4.11	3.89
Eu	2.83	1.22	1.85	1.67	1.87	1.94	1.39	1.01	1.08	1.63	1.43	1.24	1.21
Gd	7.04	4.9	4.74	9.62	4.75	5.9	5.23	3.56	2.76	4.3	6.06	3.17	3.28
Tb	1.34	1.02	0.97	2.06	1.02	1.24	1.1	0.73	0.59	0.83	1.28	0.65	0.64
Dy	6.32	5.03	4.98	10.2	4.84	5.96	5.2	3.64	2.86	4.12	6.38	2.99	2.88
Ho	1.31	1.13	1.13	2.22	1.07	1.33	1.13	0.8	0.64	0.85	1.35	0.64	0.61
Er	4.22	3.89	3.79	6.84	3.71	4.56	3.59	2.67	2.07	2.74	4.62	1.99	1.87
Tm	0.66	0.58	0.59	0.99	0.58	0.69	0.55	0.4	0.31	0.4	0.68	0.28	0.28
Yb	4.2	4.08	4.24	6.04	3.82	4.44	3.5	2.78	2.01	2.75	4.48	1.73	1.8
Lu	0.71	0.71	0.73	0.89	0.65	0.71	0.58	0.48	0.36	0.45	0.74	0.29	0.27

bdl: Below detection limit

Table 1. Continued

Sample	Granodiorite										Granite					
	45	4b	28	29	30	33	40b	39	44	47	27	10b	1a	21b	3c	4a
SiO ₂	63.84	67.7	66.5	68.2	70.5	65.9	65.7	67.7	68.7	67.9	68.8	71.8	69.8	73.9	69.7	67.6
TiO ₂	0.39	0.26	0.32	0.29	0.25	0.34	0.33	0.31	0.27	0.28	0.27	0.22	0.27	0.15	0.24	0.48
Al ₂ O ₃	16.89	14.9	16.4	15.4	15.7	15.9	16.3	16.1	15.9	16.3	15.2	14	14.7	13.3	14.2	13.2
Fe ₂ O _{3t}	5.08	4.59	3.53	4.13	2.53	4.02	4.03	4.42	2.91	3.17	3.44	2.46	1.03	2.07	4.07	5.84
MgO	1.43	0.67	1.23	0.99	0.59	0.94	1.13	0.75	0.83	0.83	0.86	0.67	0.19	0.37	0.83	1.22
MnO	0.04	0.05	0.08	0.06	0.04	0.07	0.07	0.04	0.03	0.04	0.06	0.05	0.03	0.04	0.04	0.08
CaO	3.25	1.11	3.12	3.1	1.6	3.96	3.78	2.7	2.78	2.79	1.87	1.34	3.04	1.62	2.09	1.37
Na ₂ O	4.4	3.45	4.47	4.3	4.16	4.27	4.15	4.26	3.98	4.28	4.28	3.86	3.81	3.52	3.69	2.61
K ₂ O	3.25	5.85	2.52	1.97	3.15	2.37	2.71	2.1	3.07	3.01	3.83	4.42	5.11	4.19	3.89	5.85
P ₂ O ₅	0.25	0.23	0.16	0.13	0.14	0.17	0.17	0.16	0.13	0.15	0.11	0.08	0.15	0.11	0.11	0.2
LOI	1.1	1.1	1.7	1.3	1.4	2.1	1.5	1.4	1.4	1.1	1.2	1.1	1.9	0.8	1.1	1.5
Total	99.93	99.9	100	99.9	100	100	99.9	99.9	99.9	99.9	100	100	100	100	100	99.9
Ni	10	5	4	5	1	3	4	6	2	2	3.5	1.8	1.9	1.4	6.7	5.2
Cr	bdl	20	20	20	bdl	10	10	20	bdl	bdl	10	bdl	bdl	bdl	20	10
Co	5	4	5	5	2	6	6	10	4	3	4	3	1	2	4	8
Ga	19	15	17	16	16	17	16	16	15	16	15	14	14	13	14	15
Rb	87	120	71	49	95	54	67	62	67	71	100	129	117	106	85	102
Sr	498	580	479	479	364	599	585	500	396	471	524	388	552	347	528	473
Ba	592	2072	463	428	614	611	594	328	579	557	498	485	714	380	572	1790
Zr	141	156	145	158	182	161	174	155	162	168	125	106	152	112	134	234
Nb	19.1	14	14	14	14	14	15	14	12	12	15	16	16	11	12	19
Ta	2	1	1	1	1	1	1	1	1	1	1	2	1	1	1	1
Th	6	13	6	9	15	10	12	8	10	13	16	21	16	17	14	23
U	5	4	2	4	3	2	4	1	2	4	3	9	4	2	3	3
Y	23	19	18	22	21	29	20	10	17	21	17	17	16	16	15	34
La	26.8	31	28.7	30	38.3	51.4	31.5	17.1	22.7	31.2	21.9	24.7	19.9	21.2	22.4	70.6
Ce	55.3	63.2	60.3	63	77.9	102	65.5	38.7	46.7	64.1	46.6	51	51.2	42.2	45	139
Pr	5.76	6.6	6.26	6.76	7.94	10.6	6.95	4.08	4.86	6.61	4.99	5.19	5.66	4.39	4.73	14
Nd	19.9	22.9	21.3	23.8	27.1	35.7	23.2	14.7	17	22.5	17.6	17	18.7	14.9	16.8	47
Sm	3.45	3.76	3.35	3.9	4.25	6.06	3.83	2.54	2.81	3.65	2.93	2.53	3.12	2.52	2.65	7.24
Eu	0.9	0.99	0.95	0.93	0.99	1.34	0.96	0.8	0.83	0.91	0.78	0.59	0.71	0.62	0.74	1.39
Gd	3	2.83	2.47	3	3.17	4.55	2.89	1.78	2.12	2.82	2.27	1.89	2.31	1.93	1.96	4.99
Tb	0.63	0.54	0.49	0.61	0.63	0.95	0.57	0.34	0.44	0.58	0.48	0.4	0.45	0.39	0.39	1
Dy	3.13	2.38	2.23	2.88	2.78	4.47	2.67	1.56	2.17	2.69	2.2	1.79	2.08	1.93	1.85	4.46
Ho	0.65	0.5	0.51	0.6	0.61	0.91	0.57	0.3	0.45	0.57	0.49	0.41	0.45	0.41	0.38	0.91
Er	2.12	1.62	1.58	1.91	1.95	2.6	1.82	1.01	1.5	1.9	1.6	1.46	1.4	1.37	1.29	2.91
Tm	0.28	0.25	0.24	0.29	0.3	0.39	0.28	0.16	0.23	0.31	0.26	0.25	0.23	0.21	0.2	0.41
Yb	1.89	1.61	1.58	1.81	2.01	2.31	1.82	1.04	1.55	1.9	1.8	1.68	1.54	1.41	1.37	2.63
Lu	0.3	0.28	0.26	0.31	0.35	0.36	0.3	0.19	0.25	0.34	0.31	0.32	0.26	0.25	0.24	0.44

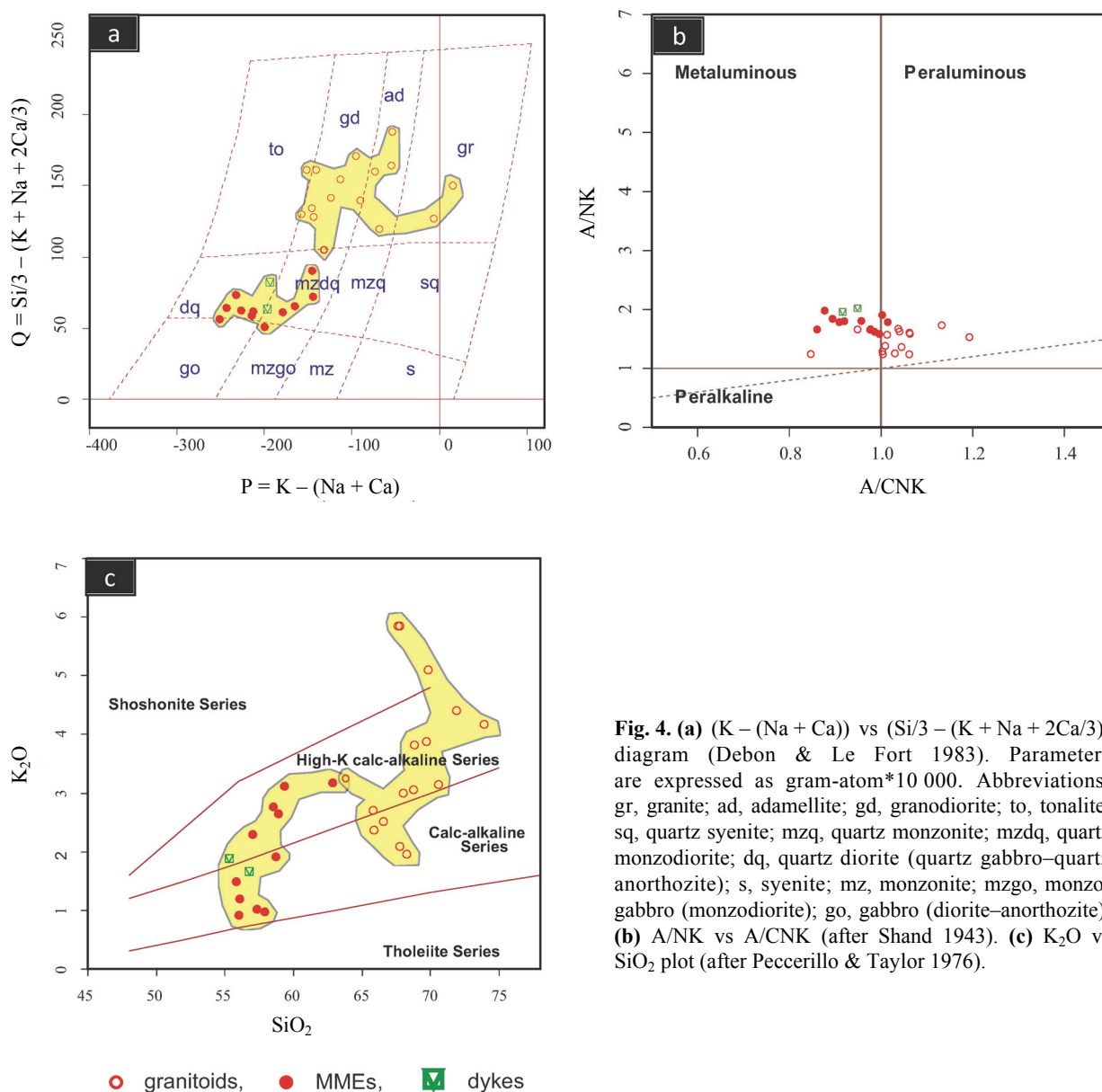


Fig. 4. (a) $(\text{K} - (\text{Na} + \text{Ca}))$ vs $(\text{Si}/3 - (\text{K} + \text{Na} + 2\text{Ca}/3))$ diagram (Debon & Le Fort 1983). Parameters are expressed as gram-atom*10 000. Abbreviations: gr, granite; ad, adamellite; gd, granodiorite; to, tonalite; sq, quartz syenite; mzq, quartz monzonite; mzdq, quartz monzodiorite; dq, quartz diorite (quartz gabbro–quartz anorthosite); s, syenite; mz, monzonite; mzgo, monzogabbro (monzodiorite); go, gabbro (diorite–anorthosite). (b) A/NK vs A/CNK (after Shand 1943). (c) K_2O vs SiO_2 plot (after Peccerillo & Taylor 1976).

minor quartz monzogabbro/monzodiorite. The chemical compositions of the greenish dyke in the HP are similar to MME, and samples of these dykes plot in the quartz monzodiorite/monzogabbro and quartz diorite/gabbro fields. In the A/NK versus A/CNK diagram (Fig. 4b), most of the samples from the HP rocks and MMEs plotted in the metaluminous field, only a few Horoz host rocks are found in the peraluminous field. All HP samples show in the high-K calc-alkaline features in the K_2O versus SiO_2 diagram (Fig. 4c). Besides, the granite member of the HP displays a slightly more potassic character by plotting within the shoshonite field.

In comparison with the MMEs and their host rocks, the greenish dyke samples show more enrichment in

MgO , Cr , Co , Pb , Sr , Ba , La and more depletion in Na_2O , Nb , Ta , Yb and Lu . With increasing SiO_2 (Fig. 5), a negative correlation exists in CaO , MgO , FeO , TiO_2 and P_2O_5 (not shown). However, the samples are scattered in SiO_2 versus trace element diagrams (Fig. 5).

The primitive mantle-normalized trace element diagrams show consistent patterns for the HP and its MMEs (Fig. 6). The dyke samples differ from the MMEs and their host in having positive Pb anomaly and no Eu anomalies. Both the host rocks and MMEs have usual consistent patterns, with well-developed negative Ba , Nb , Ti and P anomalies. Chondrite-normalized REE patterns of all rocks are light REEs (LREEs) enriched

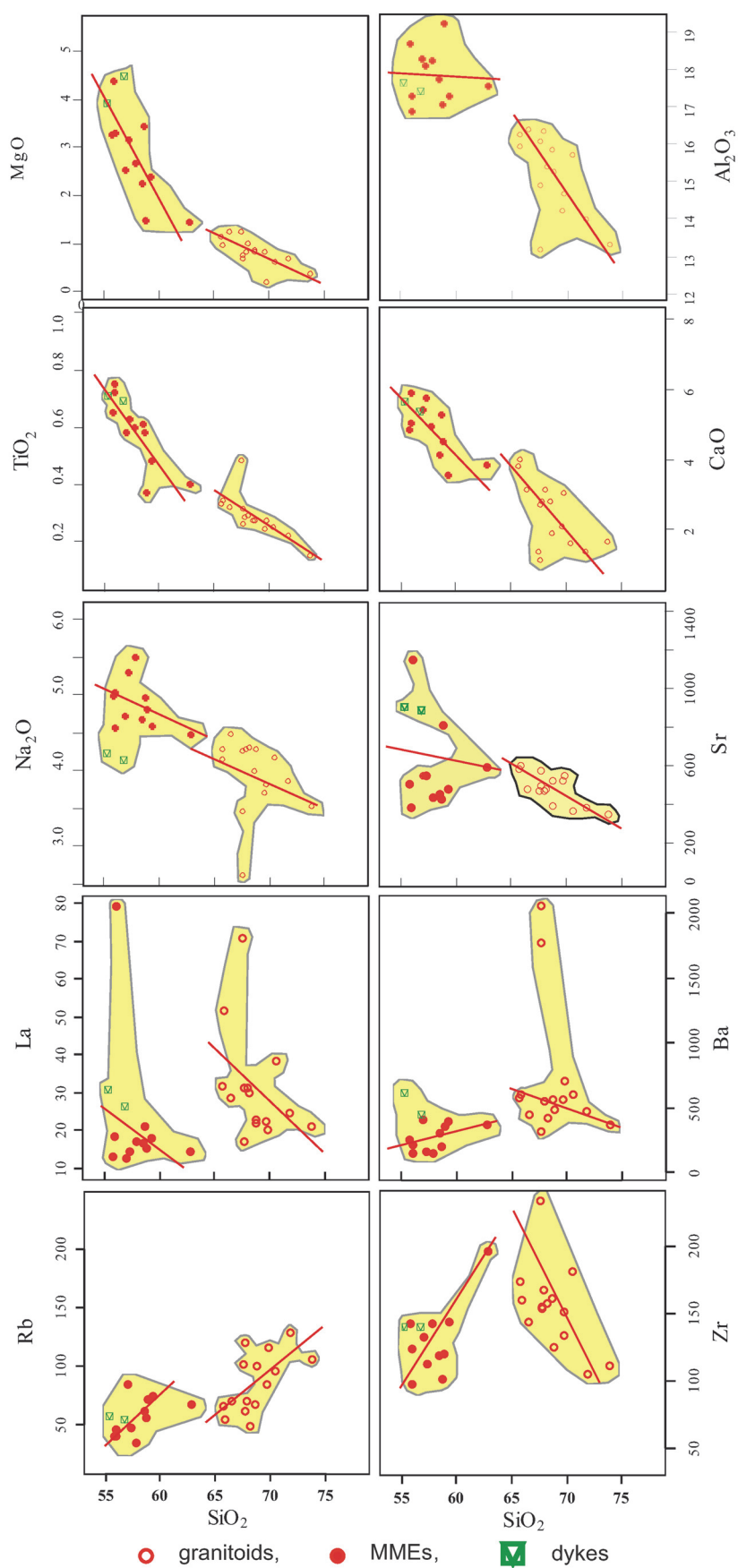


Fig. 5. Selected major and trace element Harker variation diagrams for samples from the Horoz granitoids, including dykes and enclaves.

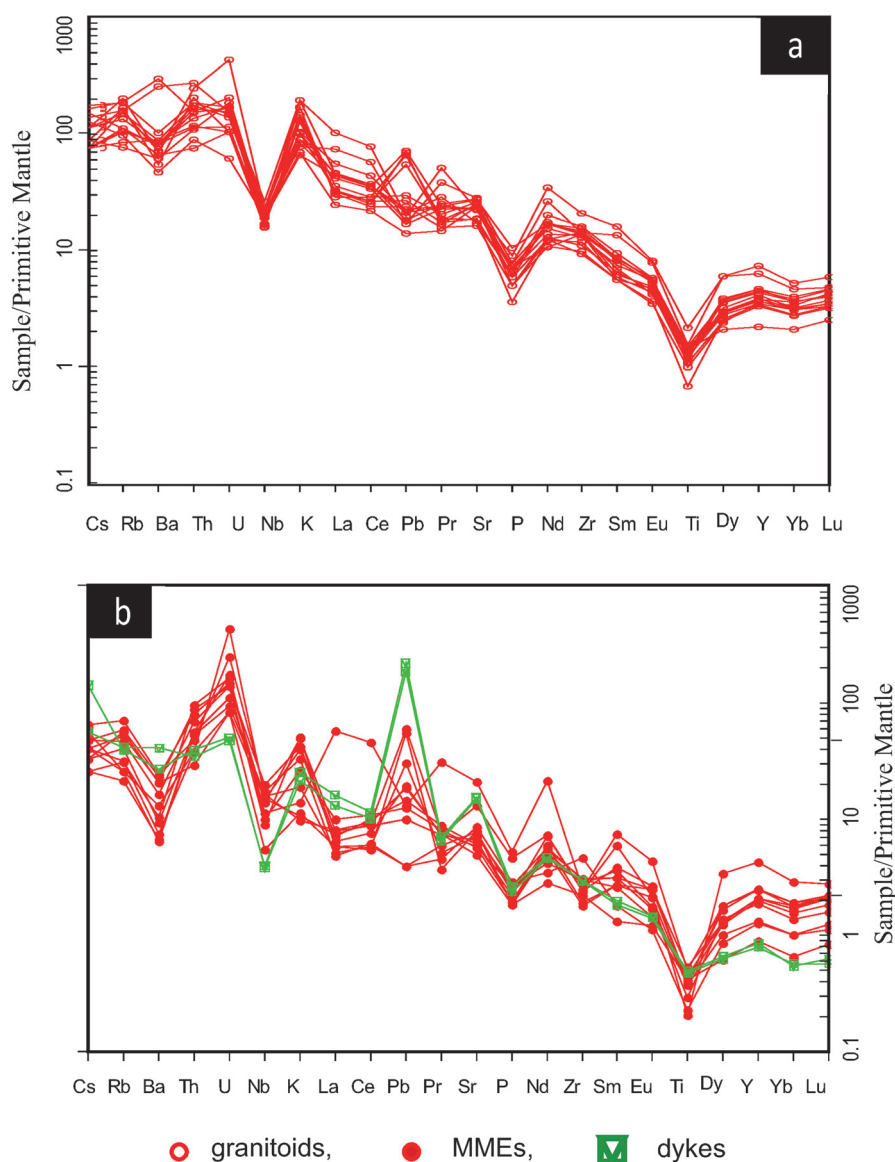


Fig. 6. Primitive mantle normalized spider diagrams of granite samples. Normalizing values are from Sun & McDonough (1989).

relative to heavy REEs (HREEs). The $(La/Yb)_N$ values of all rocks are in the same range, indicating similar sources. However, the patterns are relatively fractionated due to the fractionation of hornblende and/or feldspar phases. The REE patterns of the granitic rocks $[(La/Yb)_N 8.2–18]$ are slightly concave-upward, suggesting amphibole fractionation (Fig. 7a, b). They have negligible Eu anomalies, but a few samples display significant negative Eu anomalies (e.g. $Eu/Eu^* = 0.71$). The MMEs are less fractionated $[(La/Yb)_N 1.7–12.7]$ than the granitic rocks.

Sr–Nd–Pb isotopes

Host rocks have a low and variable initial $^{87}Sr/^{86}Sr$ ratio (0.7047) and negative epsilon values (Fig. 8a). A range of initial ratios (0.7046–0.7058) for the MMEs was obtained by calculating the measured ratios for the inferred emplacement age (50 Ma). In general, the MMEs have an initial $^{87}Sr/^{86}Sr$ ratio and Nd isotope ratios similar to those of their hosts. Host rocks and their MMEs have Nd model ages relative to a depleted mantle reservoir (T_{DM}) of 0.74–0.84 and 0.75–1.38 Ga, respectively.

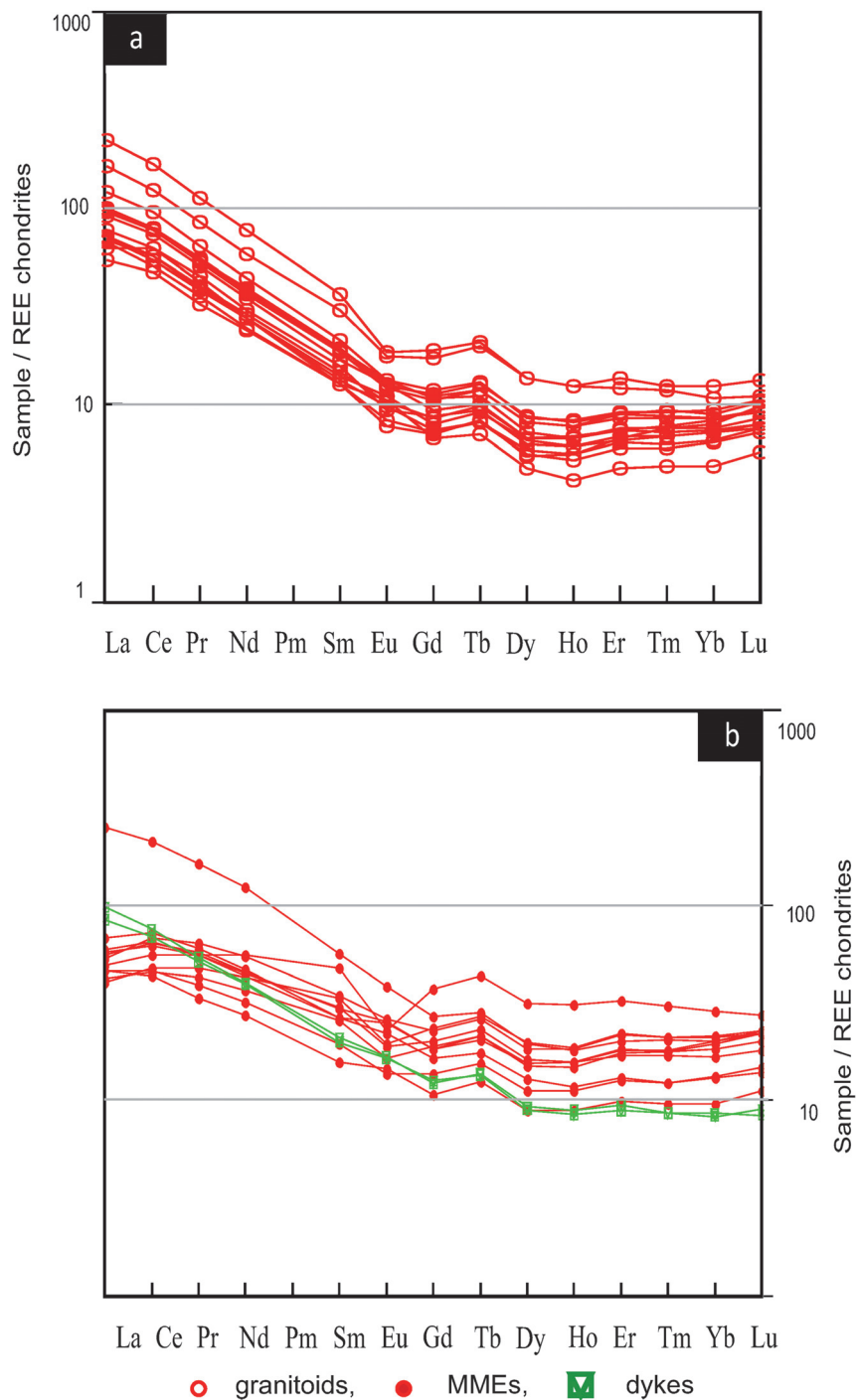


Fig. 7. Chondrite normalized rare-earth element patterns of the host rocks and their MMEs with dyke samples. Normalizing values are from Boynton (1984).

The $^{206}\text{Pb}/^{204}\text{Pb}$ ratios are between 19.333 and 19.362 in host rocks and between 19.691 and 19.829 in the enclaves. In the Pb-isotope ratios (Fig. 8b) diagram, although MME seems to plot in the mid-ocean ridge basalt (MORB) field, those samples are also at the Northern Hemisphere Reference Line (NHRL), indicating

that the subduction-related component was dominated by the material contributed by aqueous fluids rather than by sediments. The MMEs are found on the area of Pacific MORB, while host rocks plot into the field of oceanic sediments and at the boundary of enriched mantled-II.

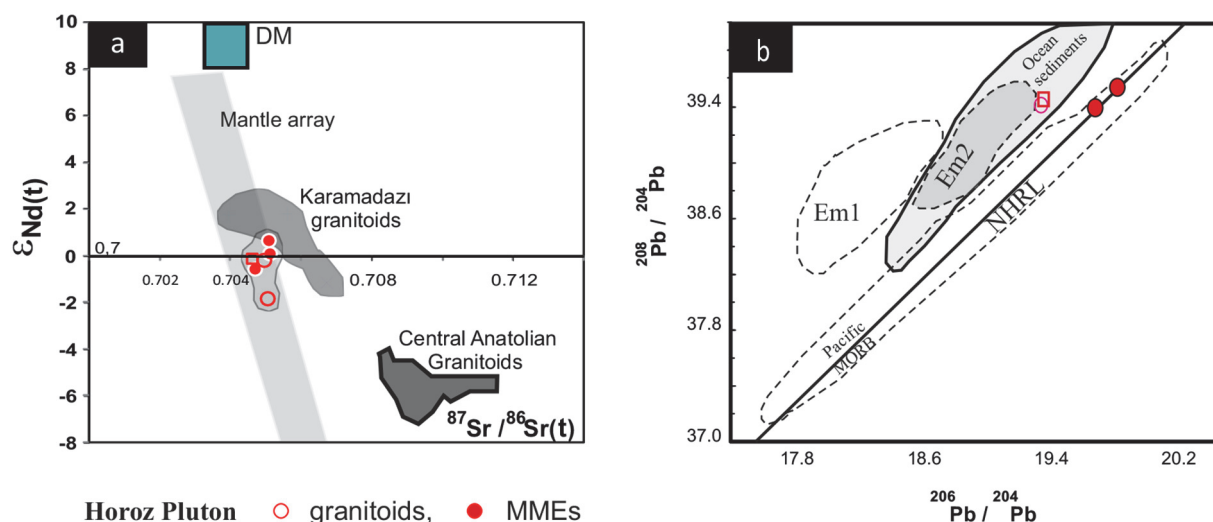


Fig. 8. (a) $(^{87}Sr/^{86}Sr)_t$ vs $\epsilon_{Nd(t)}$ plot of the Horoz and Karamadazi granitoids and their mafic enclaves. Composition fields for Karamadazi granitoids from Kocak (2008), for Central Anatolian granitoids from Ilbeyli et al. (2004). DM, depleted mantle. (b) $(^{206}Pb/^{204}Pb)$ vs $(^{208}Pb/^{204}Pb)$ variation diagram of the Horoz samples. Northern Hemisphere Reference Line (NHRL) indicated (Hart 1984).

DISCUSSION

Source characteristics and origin of the MMEs and dykes

The MMEs and dykes show low Ni (4–14 ppm and 47–53 ppm, respectively) and Cr (mostly < 30 ppm and 190–200 ppm) values, which are lower than the Ni–Cr concentrations (Ni = 250–300 ppm, Cr = 500–600 ppm) expected for a primitive basaltic magma derived from a mantle peridotite source (e.g. Wilson 1989). All these features suggest that the studied MME and dyke magmas could have undergone fractional crystallization (Taylor & McLennan 1985) and/or crustal contamination. In the MME samples, SiO_2 shows a negative correlation with MgO , FeO_b , CaO and TiO_2 , suggesting crystal fractionation of hornblende (\pm pyroxene) and Fe–Ti oxide (Fig. 5).

The MMEs and dykes have relatively low SiO_2 contents (54–63% and 55–57%) and intermediate to high molar Mg# (34–56 and 56–58), which is inconsistent with the partial melting of the mafic lower crustal rocks and requires a mantle-derived component. The Nb/Ta ratio is a good indicator of pressure, and the ratio decreases as pressure increases (Azizi et al. 2015). Accordingly, the Nb/Ta and Zr/Sm ratios of the MMEs and dyke samples can also be used to discriminate their formation under eclogite-facies or amphibolite-facies conditions (Hoffmann et al. 2011). The fairly low Nb/Ta (10–20) and Zr/Sm (11–51) ratios for the MME rocks from the HP suggest that they formed under garnet amphibolite-facies rather than under eclogite-facies conditions.

Most of the samples with no Eu anomalies accompanied by positive Sr anomalies (Fig. 6b) could reflect melting at pressures above the plagioclase stability field (>15 kbar, >~55 km) or plagioclase accumulation. The high Sr abundances (389–1149 and 892–909 ppm, respectively) in the MMEs and dykes also support this suggestion. However, the samples have high Y (23–76 and 21–22 ppm) and correspondingly low Sr/Y (9–24 and 41–42 ppm), which indicates that plagioclase was possibly in the residue. Unfractionated HREE (and Y) patterns generally suggest that the mafic magma was possibly produced outside the garnet stability field (i.e. plagioclase stable without garnet; Drummond & Defant 1990; Rapp et al. 1991; Springer & Seck 1997; Martin 1999; Pe-Piper et al. 2002). But, garnet as a residual mineral would be able to produce $(Gd/Yb)_N$ ratios > 1 (e.g. Martin 1999; Klein et al. 2000; Martin et al. 2005). Therefore garnet may exist in the source of the mafic rocks. Accordingly, the experimental melting of metabasalts under fluid-absent conditions (Rapp et al. 1991; Rapp & Watson 1995) indicates that pressures >0.8 GPa are required to stabilize garnet, and ≥ 1.2 GPa for garnet thoroughly replaces plagioclase. Alternatively, most of the mafic rocks may have been derived from sources located at depths between 30 and 44 km by assuming 1 kbar = 3.7 km for the continental crust (Tulloch & Challis 2000). The amphiboles from the enclaves yield a maximum pressure of 4.1 ± 0.6 kbar at 730 °C (Kocak et al. 2011), suggesting the crystallization of the mafic magma at least at 15 km.

The existence of the greenish-coloured dyke resembling enclaves in adjacent granitoids in the HP may suggest that the magma of the MMEs can exist either independently of, or as a separate layer in, their host granitoid magma bodies. In general, the dykes exhibit a similar pattern to that of the host rocks, with a high $(La/Lu)_N$ ratio (10.4–11.3). In comparison with the scattered smaller MMEs, the dykes seem to be less differentiated (more enrichment in MgO, Cr, Co), but more enriched in Pb, Sr, Ba and LREEs. This may indicate either distinct parental magmas, or different mechanisms or degrees of interaction of the mafic magma with the partially crystallized host-granite, or both. Along with their identical occurrences with the MMEs, this precludes that the dykes correspond to several pulses of mafic magmas. The higher content of large ion lithophile elements (LILEs) and LREEs in the dykes could suggest stronger interactions with the granites, diffusion of water and alkalis, etc. A pronounced negative Nb, P, Ti anomaly (Fig. 6b) may also support this suggestion.

Magma mixing versus restites or autoliths

Based on their mafic composition, the MMEs could have a cumulate or autolith origin (e.g. Noyes et al. 1983; Chappell et al. 1987; Clemens & Wall 1988; Shellnutt et al. 2010; Dahlquist 2002; Donaire et al. 2005), which ignores the grain size differences between the MMEs and host granitoids. Some major and trace elements, such as Al_2O_3 , Na_2O , Rb, Ba, Sr and Zr (Fig. 5) exhibit non-linear variations. Among these, SiO_2 versus Ba and Sr (Fig. 5) is of particular interest, in which Ba and Rb contents change significantly for little change in SiO_2 in the MMEs. Dispersion on the diagrams is of paramount evidence of biotite ‘cumulus’. The small amount of biotite may induce an increase in Ba and Rb contents in mafic samples due to their high partition coefficients (K_D) for Ba (6.36, Philpotts & Schnetzler 1970) and for Rb (3.53, Matsui et al. 1977). Plagioclase and K-feldspar have low K_D for Ba (0.36, López-Ruiz & Cebriá 1990) and for Rb (0.07–0.76, Icenhower & London 1996), respectively, therefore they are unlikely to cause this enrichment. However, the MMEs are fine-grained, 10 to 20 times smaller in comparison with the same phases in the host granitoid and have low Ni and Cr, which suggests that the enclaves as a whole cannot be a cumulate of the pluton itself. It is also remarkable that all the enclaves and host rocks have similar total REE concentrations and sub-parallel REE patterns, which are inconsistent with the autolith model. The presence of MMEs in the granitoids could also be indicative of the evolution of the HP through the restite unmixing mechanism (Chappell et al. 1987; Chen et al. 1989; Chappell & White 1992; Chappell 1996; White et al. 1999). The

field characteristics of the MMEs, and lack of linear trends for K_2O (Fig. 4c), Ba, La, Zr with SiO_2 (Fig. 5) exclude restite origin. Therefore, the MMEs in the studied HP could have developed mostly by mingling/mixing between near-contemporaneous mafic and felsic magmas (e.g. Vernon 1984; Wiebe et al. 1997; Barbarin 2005; Hawkesworth & Kemp 2006; Kocak 2006; Feeley et al. 2008; Chen et al. 2009; Kocak et al. 2011; Liu et al. 2013).

The magma mixing process could take place before or after the injection of the enclave-forming magma into the felsic host magma. Since the MME samples are mostly non-porphyrific, fine-grained and enclosed in another enclave, the mixing process probably happened prior to the injection of the enclave-forming magma. Furthermore, the mafic enclaves are characterized by relatively low Mg, Ni and Co, suggesting that they were much evolved before their injection into the host felsic magmas. This implies that significant fractionation of hornblende (\pm pyroxene) had occurred before and during the process of crustal contamination/magma mixing at depth. The MMEs are characteristically enriched in P, Ti, Y, Nb, and HREEs, possibly due to selective inter-diffusion of these elements into the less polymerized magmas. These elements were consequently concentrated in apatite, titanite and hornblendes due to their high K_D for these elements (López-Ruiz & Cebriá 1990; Klein et al. 1997), keeping their low activity in the melt. Such low activity in the mafic melt gives rise to the continuity of ‘Uphill’ diffusion, as described for K due to crystallization of biotite by Johnston & Wyllie (1988). Selective diffusion of these elements may be attributed to the crystallization of biotite as cumulate. The Ba depletion in most enclaves could be connected to the complicated feldspar transfer processes at the contact with host magmas and somewhat to the dilution effect induced by the inward migration of Si and alkalis as suggested by some researchers (Bussy 1991; Debon 1991; Orsini et al. 1991).

In general, MME samples have higher ϵ_{Nd} than their hosts (Fig. 8a, Table 2), suggesting isotopic equilibration between mafic and felsic magmas, which is usually more easily achieved than chemical equilibration since isotopic exchanges proceed more quickly than chemical exchanges (Leshner 1990). The MMEs have generally $^{87}Sr/^{86}Sr$ values close to or in the range of that for the respective host granite, suggesting a granite–enclave interaction (Fourcade & Javoy 1991). The MMEs and host rocks have distinct $^{206}Pb/^{204}Pb$, but similar $^{208}Pb/^{204}Pb$ values (Fig. 8b). Small variations in the amount and composition of Pb contributed to the mafic melt by the relatively elevated $^{206}Pb/^{204}Pb$ of zircon compared to $^{208}Pb/^{204}Pb$ would result in large relative changes in $^{206}Pb/^{204}Pb$ with only small changes in $^{208}Pb/^{204}Pb$.

Table 2. Results of the whole-rock Sr, Nd and Pb isotope analyses of the enclave and hosts

Sample	$^{87}\text{Rb}/^{86}\text{Sr}$	$^{87}\text{Sr}/^{86}\text{Sr}$	$^{87}\text{Sr}/^{86}\text{Sr}(t)$	$^{147}\text{Sm}/^{144}\text{Nd}$	$^{143}\text{Nd}/^{144}\text{Nd}$	$\epsilon_{\text{Nd}(t)}$	TDM (Ga)	$^{206}\text{Pb}/^{204}\text{Pb}$	$^{207}\text{Pb}/^{204}\text{Pb}$	$^{208}\text{Pb}/^{204}\text{Pb}$	
Enclaves	17b	0.4480	0.7050	0.7047	–	–	–	–	–	–	
	21a	0.2475	0.7059	0.7058	–	–	–	–	–	–	
	13a	0.3691	0.7054	0.7051	0.12458	0.5126	0.1	0.91	–	–	
	24a	0.3790	0.7054	0.7051	0.1107	0.5126	0.7	0.75	19.829	15.751	39.543
	40a	0.4484	0.7050	0.7047	0.15255	0.5126	–0.6	1.38	19.691	15.731	39.395
Granite	21b	0.8855	0.7052	0.7046	0.10225	0.5126	–0.2	0.75	19.362	15.718	39.466
Granodiorite	40b	0.3295	0.7052	0.7050	0.09981	0.5126	–0.2	0.74	19.333	15.712	39.430
	47	0.4370	0.7054	0.7051	0.09807	0.5125	–1.8	0.84	–	–	–
	29	0.2951	0.7050	0.7048	–	–	–	–	–	–	–
	45	0.5085	0.7055	0.7051	–	–	–	–	–	–	–

Sr- and Nd-isotope initial ratios calculated at 50 Ma. TDM values calculated using present-day $(^{147}\text{Sm}/^{144}\text{Nd})_{\text{CHUR}} = 0.1967$ and $(^{143}\text{Nd}/^{144}\text{Nd})_{\text{CHUR}} = 0.512638$.

CHUR: Chondritic Uniform Reservoir.

–, No analyses.

Source characteristics and genesis of the host granitic rocks

The host granitic rocks are characterized by pronounced negative Nb, Ba, P and Ti anomalies but are enriched in Rb, Th and K. These features are in accordance with those of typical crustal melts, e.g., Himalayan granites (Harris et al. 1986) and granitoids of the Lachlan Fold belt (Chappell & White 1992), and the subduction component. However, the host rocks have relatively low $\text{Sr}(t)$ (0.7067) and high $\epsilon_{\text{Nd}(t)}$ values (–0.2 to 1.8) (Table 2, Fig. 8a), suggesting mantle material involved in the generation of the HP. Similarly, the MMEs in general, have an initial $^{87}\text{Sr}/^{86}\text{Sr}$ ratio and Nd isotope ratios similar to those of their hosts, suggesting significant input of a lithospheric mantle-derived component during magma generation. The granitoids show high-K–shoshonitic and I-type characteristics with a wide range of silica content ($\text{SiO}_2 = 64\text{--}74$ wt%), relatively low-intermediate Mg# (22–41) and low Ni content (1.4–10.0 ppm), all of which may indicate that they could be developed from the mixing of the lower crust and mantle-derived magmas (e.g. Barbarin 1999). Hence average Nb/Ta ratios are 17.5 for mantle-derived and 11–12 for crustal-derived magmas (Green 1995), Nb/Ta ratios for the felsic samples vary between 10.05 and 18.12, suggesting crustal- and mantle-derived magmas in the generation of the HP.

Both MMEs and felsic samples show colinear variation in the Harker diagrams, suggesting that the host granites and MMs/dykes are possibly variably differentiated products of the same parent magma which derived from mixing melts of lithospheric mantle and crustal components. SiO_2 increases with decreasing MgO,

FeO , CaO and TiO_2 and P_2O_5 , suggesting fractionation of hornblende (\pm pyroxene), Fe–Ti oxide and apatite. Amphibole has a high K_D for heavy REEs, but even higher for the medium and heavy REEs (such as Dy); therefore, amphibole fractionation can be traced by decreasing Dy/Yb ratios with differentiation (Davidson et al. 2007a, 2007b, 2008). Accordingly, the amphibole fractionation is indicated by concave-upward REE patterns without significant Eu anomalies (see Tepper et al. 1993, Fig. 7a, b). In the host rocks, Zr and P_2O_5 show negative correlation with SiO_2 , suggesting zircon and apatite fractionation. Aplitic suites on the HP most probably represent such comagmatic highly differentiated late-stage melts.

The existence of MMEs with mode of occurrence and mineralogical (Kocak et al. 2011) and geochemical characteristics suggest mafic–felsic interaction and mingling (Barbarin & Didier 1992; Barbarin 1999; Ferré & Leake 2001; Kocak 2006) by the injection of hot mafic magma into felsic magma (source mixing). Langmuir et al. (1978) showed that in the ratio–ratio and ratio–element plots, data consistent with mixing lie along a hyperbolic curve for both isotopic and elemental ratios, while a linear array forms when the ratios of the concentrations of the two denominators are the same for all data points. In the samples, these characteristic hyperbolic mixing arrays are observed in plots of $\text{Al}_2\text{O}_3/\text{CaO}$ versus $\text{Na}_2\text{O}/\text{K}_2\text{O}$, Ti/Ba versus Ti, and a linear trend is observed in a plot of $\text{Al}_2\text{O}_3/\text{CaO}$ versus $\text{Na}_2\text{O}/\text{CaO}$ (Fig. 9a–c). Accordingly, mafic (lithospheric mantle) and felsic (crustal component) magma mixing may alter both the elemental and isotopic compositions of magmas prior to the assimilation/fractionation processes.

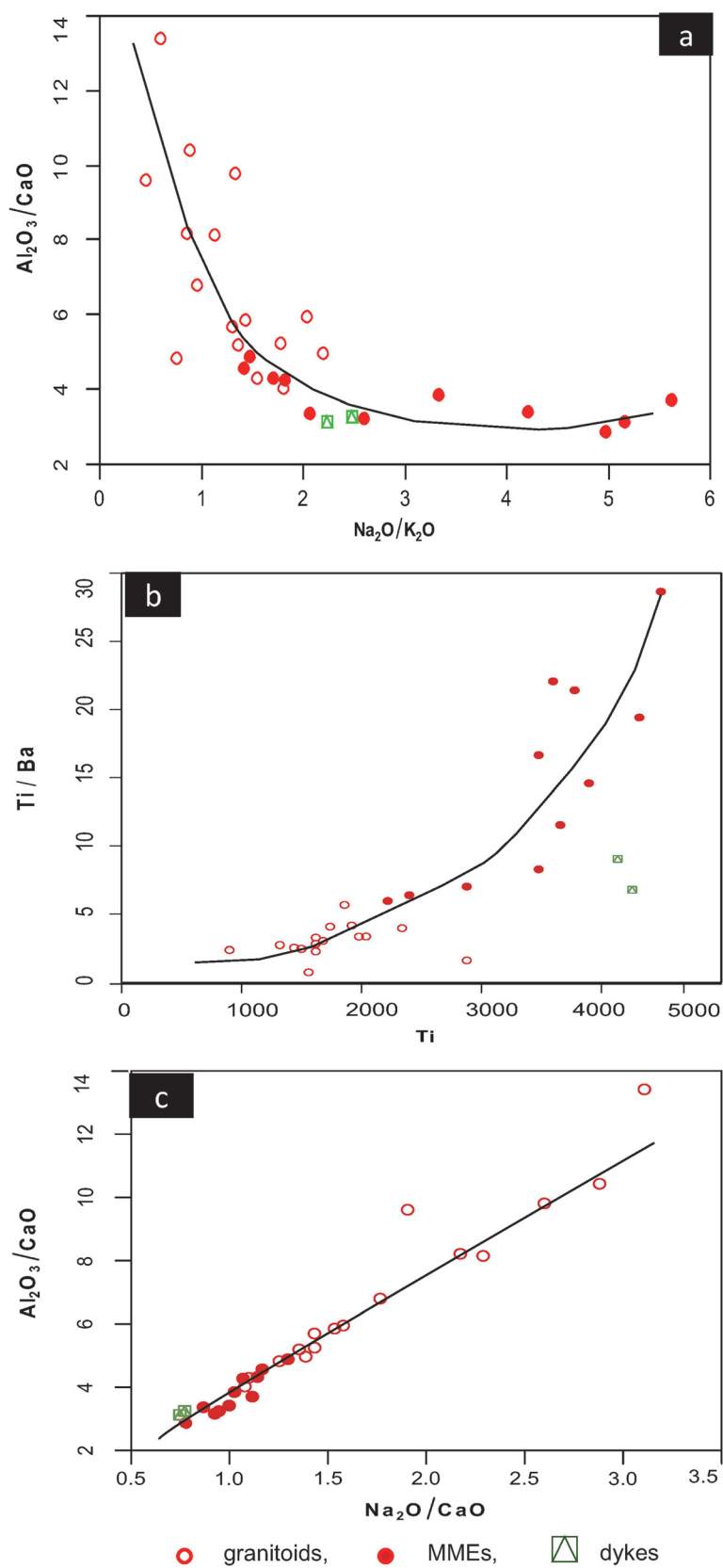


Fig. 9. Ratio-ratio (a and c) and ratio-element (b) plots.

It has also been suggested that I-type granites most likely form by the mixing of crustal materials and mantle-derived magmas rather than by the remelting of ancient meta-igneous crustal rocks (Kemp et al. 2007; Li et al. 2009; Zhu et al. 2009; He et al. 2010). Besides, relative heterogeneity of the initial Sr ratios (0.7046–0.7051) in the host rocks could be attributed to a difference in the degree of contamination of magmas with upper crustal materials.

Adakitic versus TTG

Kadioglu & Dilek (2010) suggested that the HP shows chemical characteristics of high-Al adakitic compositions, which could have formed by the partial melting of the hydrated lithospheric mantle and the amphibolitic mafic lower crust that was triggered by delamination-induced asthenospheric upwelling. However, all samples from the HP usually have lower Mg# [(molar $100 \times \text{MgO}/(\text{MgO} + \text{FeO}) < 0.41$], Ni (~4 ppm) and Cr (~9 ppm) (Fig. 10a), and higher K (~3.6 wt%), Ba (~712 ppm) and Rb (~86 ppm) contents than that of adakites. The samples have also high Sr contents and are found on the TTG area, rather than on the arc one in Fig. 10b.

It is widely accepted that TTG magmas were created by the partial melting of hydrous metabasaltic rocks transformed into garnet-bearing amphibolite or eclogite, under a variety of fluid conditions (Sen & Dunn 1994; Zamora 2000). Experimental studies show that the partial melting of the mafic lower crust could produce metaluminous granitic magmas regardless of the degree of

melting (Sen & Dunn 1994; Wolf & Wyllie 1994; Rapp & Watson 1995). High abundances of Al_2O_3 (≥ 19 wt%) in an amphibolite-derived liquid are the result of high H_2O (water-saturated) and/or high anorthite contents in the mafic protolith source (e.g. fig. 13 in Beard & Lofgren 1991; fig. 9 in Wolf & Wyllie 1994). Nevertheless, host rocks have lower Al_2O_3 contents (13.17–16.4 wt%) than the liquids developed during H_2O -saturated amphibolite partial melting experiments. Accordingly, granitoids from the HP were possibly formed under fluid-absent/vapour-absent conditions (with the only H_2O derived from the breakdown of hydrous minerals) and/or low anorthite contents in the mafic source. Figure 11 shows that the granitoids, particularly granites, could have formed by low-pressure (100–700 MPa), 20–50% dehydration melting of a basaltic/amphibolitic source. Both the mafic rocks and dykes contain high Al_2O_3 and plot (Fig. 11) between the fields of ‘low water basalt melting’ and ‘1000 Mpa, no-water melting of a basaltic/amphibolitic source’, suggesting relatively higher-pressure conditions in comparison with their host rocks during the partial melting event.

The TTGs require two main mechanisms to account for their petrogenesis: (1) the partial melting of the subducted oceanic crust (i.e. slab melts) in a convergent margin with usually higher Mg# values and Cr and Ni concentrations (e.g. Martin 1986, 1999; Drummond & Defant 1990; Foley et al. 2002; Kamber et al. 2002; Smithies et al. 2003) due to the interaction of the slab-derived melt with the overlying mantle wedge during ascent (Rapp et al. 1999) or (2) the melting of the

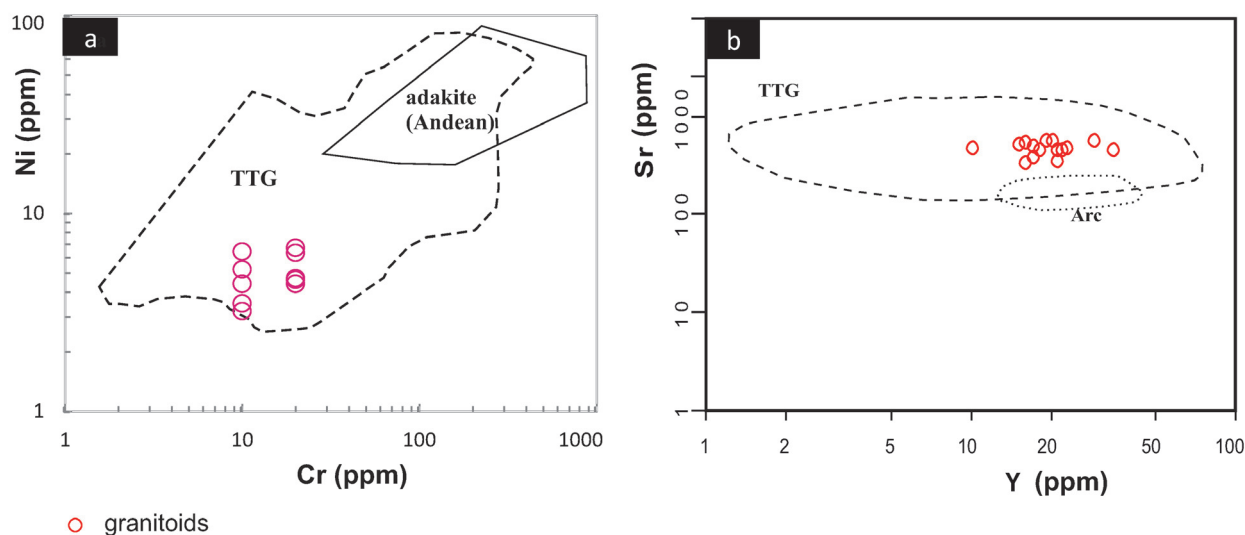


Fig. 10. (a) Cr vs Ni variation plots for granitoids. Boundaries of tonalites–trondhjemites–granodiorites (TTGs) and adakite fields are from Condie (2005). (b) Sr vs Y diagram. Archaean TTGs (Martin & Moyen 2002); ‘ordinary’ arc magmas (GEOROC project, <http://georoc.mpch-mainz.gwdg.de/georoc>).

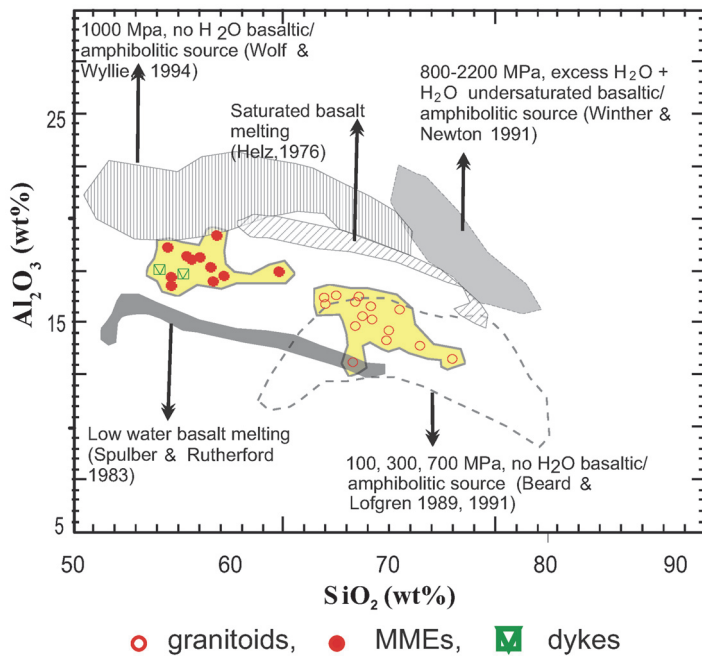


Fig. 11. SiO₂ (wt%) vs Al₂O₃ (wt%) diagram showing a possible source for the intrusions.

thickened mafic crust or underplated basalt with low Mg# values and low Cr and Ni concentrations (e.g. Atherton & Petford 1993; Petford & Atherton 1996; Rapp et al. 1999; Smithies 2000; Condie 2005; Smithies et al. 2009). In Fig. 12a, b, samples fall mostly in the field of adakites derived from the partial melting of the thick lower crust and metabasaltic and eclogite fields, rather than in that of adakite rocks derived from the partial melting of the delaminated lower crust. The data for adakites

worldwide exhibit that typical slab melts have low Rb/Sr ratios (0.01–0.05); this is in contrast with the wide range of Rb/Sr ratios (0.01–0.4) for the adakitic rocks that developed from the thickened continental lower crust (Huang et al. 2009). Hence, the relatively higher Rb/Sr ratios (0.09–0.3 in host rocks, 0.04–0.16 in MMEs) of the samples from the HP are in accordance with their derivation from the thickened lower continental crust.

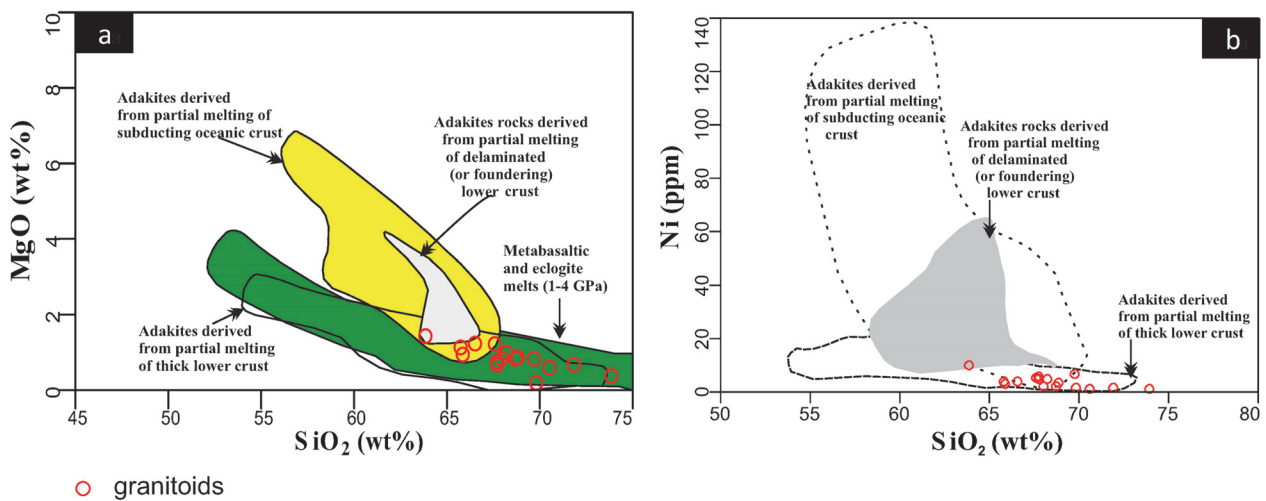


Fig. 12. (a) SiO₂ vs Mg# for the felsic rocks. Boundaries are from Rapp et al. (1999) and Smithies & Champion (2000). (b) SiO₂ vs Ni. Boundaries are from Wang et al. (2006).

Tectonic setting

I-type post-collisional granitoids with mantle-crust signature develop in many tectonic settings, such as intracontinental rifting (Vorontsov et al. 2004; Li et al. 2005; Shu et al. 2005), back-arc basins (Hochstaedter et al. 1990; West et al. 2004), island arc (Geist et al. 1995; Qian & Wang 1999), active continental margins (Donnelly & Rogers 1980) and the rifting of the passive margin (Oberc-Dziedzic et al. 2005). All MMEs and greenish dyke have lower Nb/U (average 5.9 and 5.1) than an average continental crust (Nb/U = 8.4; Rudnick & Fountain 1995). Both MMEs and granitic rocks are characterized by pronounced negative Nb anomalies, positive Pb anomalies (Fig. 6) and enrichment in LILEs and LREEs. The negative anomalies in Nb, Ti and P are characteristic of subduction-related magmas, usually thought to have resulted from the relative enrichment of the mantle source by influx of LILEs through slab dehydration (e.g. McCulloch & Gamble 1991). Similarly,

the host granite displays spikes in Cs, Rb, K and troughs in Nb and Ti (Fig. 6), which may represent the continental crust developed by the chemical differentiation of arc-derived magmas (Taylor & McLennan 1995). Besides, low La/Th (1.2–5.1) and medium-high Ba/Nb (24–145) are also typical for the rocks formed in relation with the subduction zone (Sun 1980).

The most mafic compositions in the granite (lowest in SiO₂, and highest in MgO and Co) have the highest K₂O and Na₂O contents as well as anomalously high LREE, P, Zr and Th contents and slight negative Eu anomalies, which are characteristic of A-type granites. However, they differ from A-type granites in their unelevated Rb/Sr contents or intermediate-high Ca and Sr contents (Kemp & Hawkesworth 2003) as well as unelevated Zr + Nb + Ce + Y contents (mostly <350 ppm).

In the plot of Y + Nb versus Rb of Pearce et al. (1984), all granitoid samples are clearly found in ‘post-orogenic granite’ (POG) fields (Fig. 13a). In the plot of SiO₂ versus Rb/Zr (Harris et al. 1986), the samples are

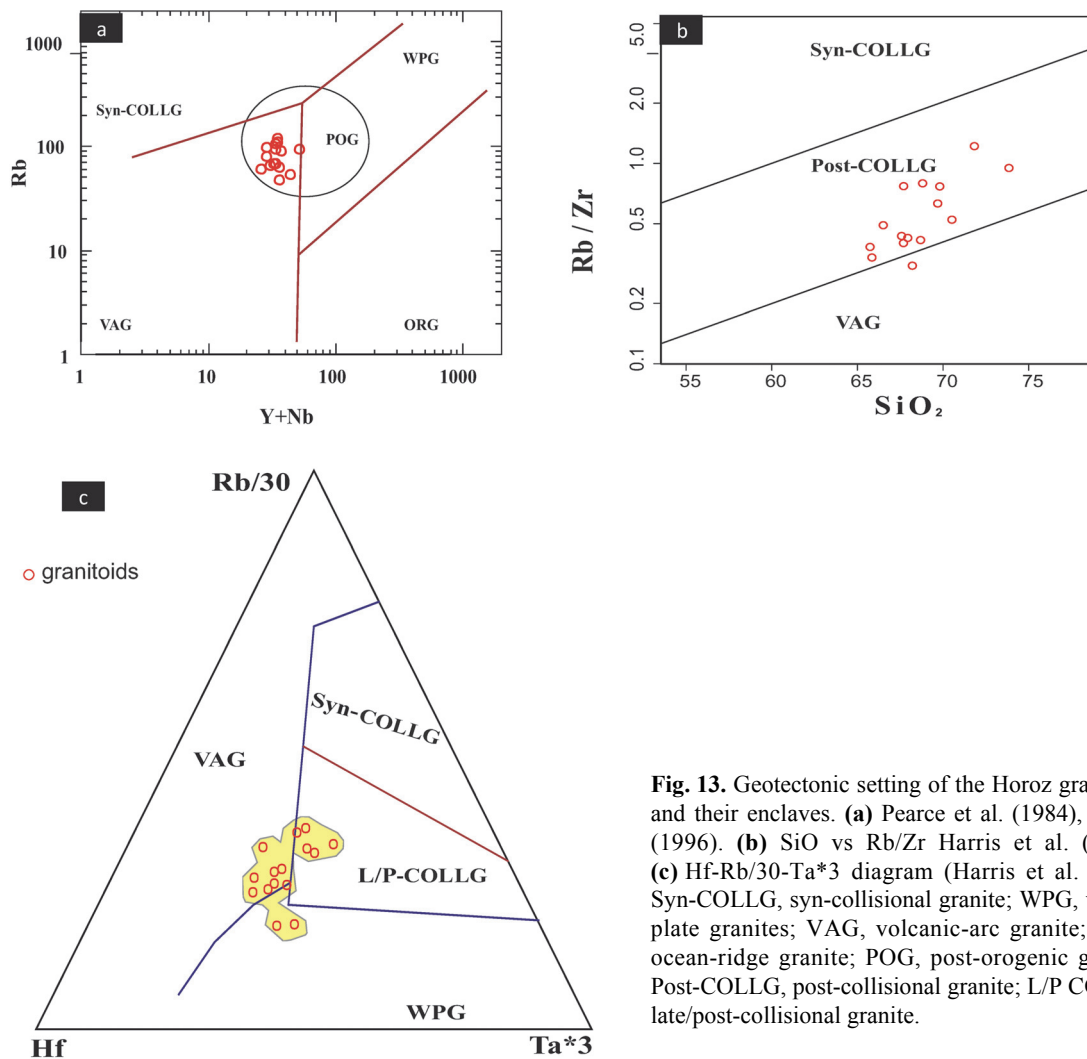


Fig. 13. Geotectonic setting of the Horoz granitoids and their enclaves. (a) Pearce et al. (1984), Pearce (1996). (b) SiO vs Rb/Zr Harris et al. (1986). (c) Hf-Rb/30-Ta*3 diagram (Harris et al. 1986). Syn-COLLG, syn-collisional granite; WPG, within-plate granites; VAG, volcanic-arc granite; ORG, ocean-ridge granite; POG, post-orogenic granite; Post-COLLG, post-collisional granite; L/P COLLG; late/post-collisional granite.

also concentrated in the ‘post-collisional’ (Post-COLLG) area in Fig. 13b. In the Harris et al. (1986) Hf–Rb/30–Ta*3 triangle (Fig. 13c), the samples straddle mostly the boundary of the volcanic-arc granite (VAG) and L/P-COLLG fields, showing a trend to the L/P-COLLG, which is similar to the other granitoids of the CACC (Goncuoglu et al. 1991; Akiman et al. 1993; Boztug 1998, 2000; Kadioglu et al. 2003, 2006; Isik & Kocak 2005; Boztug et al. 2007).

GEODYNAMIC IMPLICATION

Horoz granitoids have lower radiogenic ($^{87}\text{Sr}/^{86}\text{Sr} = 0.7045\text{--}0.7051$) and higher ε_{Nd} values (-0.085 to -1.75) than granitoids from the CACC ($^{87}\text{Sr}/^{86}\text{Sr} = 0.7080\text{--}0.7096$; $\varepsilon_{\text{Nd}} = -4.8, -6.7$, Ilbeyli et al. 2004), probably owing to a combination of upper crustal contamination and heterogeneity of the magma source. Large differences in isotopic data of granitoids from the HP and Karamadaz pluton, and granitoids from the CACC may imply that two groups of magma developed in relation with the closure of the Inner Tauride Ocean and the Izmir–Ankara–Erzincan Ocean, respectively (Kocak 2008). The Inner Tauride Ocean started to develop as early as the Jurassic between the CACC to the east and the Taurides to the west, and consumed by an intra-oceanic subduction northwards (Gorur et al. 1998) along the Inner-Tauride Suture Zone during the latest Cretaceous to early Cenozoic times. Parlak et al (2013b) suggest that the HP could have been formed as a result of hard collision (continent–continent collision) after soft collision (collision of the passive margin with the subduction trench and subsequent slab break-off). However, we suggest that the HP was emplaced after the last stage of oceanic subduction, or at a hiatus of the oceanic subduction at ~ 50 Ma. The pluton then possibly underwent cooling in two main pulses, $\sim 38\text{--}31$ Ma and late Miocene (Whitney et al. 2015).

CONCLUSIONS

From combined field, geochemical and isotopic studies it has been concluded that the mantle-derived mafic magmas from which the MMEs crystallized were likely mostly formed by mafic–felsic interaction and mingling, or prior to the mixing crystal fractionation of hornblende (\pm pyroxene) and Fe–Ti oxide. The MMEs usually underwent geochemical and Nd–Sr isotopic equilibration with their host granitoids, with resultant K, P, Ti, Y, Nb and HREE enrichments. The greenish dykes are distinct from the MMEs and display stronger interactions with the granites.

The granitoids have both crustal (distinct negative Nb, Ba, P and Ti anomalies but enriched in Rb, Th and K) and lithospheric mantle [low $\text{Sr}_{(0)}$ (0.7067) and high $\varepsilon_{\text{Nd}(0)}$ values (-0.2 to 1.8)] geochemical and isotopic signatures. They exhibit geochemical characteristics of TTGs, which were possibly created by the dehydration melting of a basaltic/amphibolitic source in a thickened lower crust. The parental granitic magma underwent the mixing of mantle-derived mafic magma and crustal felsic magma, coupled with fractional crystallization during magma ascent before emplacement. Relative heterogeneity of the initial Sr ratios (0.7046–0.7051) in the granitoids could also indicate contamination of magmas with upper crustal materials.

The HP granitoids differ from granitoids of the CACC in their lower radiogenic ($^{87}\text{Sr}/^{86}\text{Sr} = 0.7045\text{--}0.7051$) and higher ε_{Nd} values (-0.085 to -1.75), in relation with the combination of upper crustal contamination and/or heterogeneity of the magma source.

Acknowledgements. This work was financially supported by the Office of Scientific Research (BAP; Project No. 5401041, Selcuk University, Turkey). The authors are grateful to Mehmet Arslan and Alvar Soesoo for their helpful comments and suggestions on the manuscript.

REFERENCES

- Akiman, O., Erler, A., Goncuoglu, M. C., Gulec, N., Geven, A., Tureli, T. K. & Kadioglu, Y. K. 1993. Geochemical characteristics of granitoids along the western margin of the Central Anatolian Crystalline Complex and their tectonic implications. *Geological Journal*, **28**(3–4), 371–382.
- Alan, İ., Şahin, Ş., Keskin, H., Altun, İ., Bakırhan, B., Balcı, V., Böke, N., Saçlı, L., Pehlivan, Ş., Kop, A., Haniçili, N. & Çelik, Ö. F. 2007. *The Geodynamic Evolution of the Intermediate Taurus Zone: Ereğli (Konya)–Ulukışla (Nigde)–Karsantı (Adana)–Namrun (İçel) Surroundings*. MTA Report, Ankara.
- Anderson, J. A. C., Price, R. C. & Fleming, P. D. 1998. Structural analysis of metasedimentary enclaves: implications for tectonic evolution and granite petrogenesis in the southern Lachlan Fold Belt, Australia. *Geology*, **26**(2), 119–122.
- Arslan, M. & Aslan, Z. 2006. Mineralogy, petrography and whole-rock geochemistry of the Tertiary granitic intrusions in the Eastern Pontides, Turkey. *Journal of Asian Earth Sciences*, **27**(2), 177–193.
- Atherton, M. P. & Petford, N. 1993. Generation of sodium-rich magmas from newly underplated basaltic crust. *Nature*, **362**(6416), 144–146.
- Aydogan, M. S., Coban, H., Bozcu, M. & Akinci, O. 2008. Geochemical and mantle-like isotopic (Nd, Sr) composition of the Baklan Granite from the Muratdagi Region (Banaz, Uşak), western Turkey: implications for input of juvenile magmas in the source domains of

- western Anatolia Eocene-Miocene granites. *Journal of Asian Earth Sciences*, **33**(3–4), 155–176.
- Azizi, H., Zanjefili-Beiranvand, M. & Asahara, Y. 2015. Zircon U–Pb ages and petrogenesis of a tonalite–trondhjemite–granodiorite (TTG) complex in the northern Sanandaj–Sirjan zone, northwest Iran: Evidence for Late Jurassic arc–continent collision. *Lithos*, 216–217, 178–195.
- Bacon, C. R. 1986. Magmatic inclusions in silicic and intermediate volcanic rocks. *Journal of Geophysical Research: Solid Earth*, **91**(B6), 6091–6112.
- Barbarin, B. 1999. A review of the relationships between granitoid types, their origins and their geodynamic environments. *Lithos*, **46**(3), 605–626.
- Barbarin, B. 2005. Mafic magmatic enclaves and mafic rocks associated with some granitoids of the central Sierra Nevada batholith, California: nature, origin, and relations with the hosts. *Lithos*, **80**(1–4), 155–177.
- Barbarin, B. & Didier, J. 1992. Genesis and evolution of mafic microgranular enclaves through various types of interaction between coexisting felsic and mafic magmas. *Transactions of the Royal Society of Edinburgh, Earth Sciences and Environmental*, **83**(1–2), 145–153.
- Beard, J. S. & Lofgren, G. E. 1989. Effect of water on the composition of partial melts of greenstone and amphibolites at 1, 3 and 6.9 kb. *Science*, **244**(4901), 195–197.
- Beard, J. S. & Lofgren, G. E. 1991. Dehydration melting and water-saturated melting of basaltic and andesitic greenstones and amphibolites at 1, 3 and 6.9 kb. *Journal of Petrology*, **32**(2), 365–401.
- Bédard, J. 1990. Enclaves from the A-type granite of the Mégantic Complex, White Mountain magma series: clues to granite magmagenesis. *Journal of Geophysical Research*, **95**(B11), 17797–17819.
- Bingöl, E. 1974. 1/2,500,000 ölçekli Türkiye metamorfizma haritası ve bazı metamorfik kusakların jeotektonik evrimi üzerine tartışmalar [Discussion on the metamorphic map in a scale of 1:2,500,000 and geotectonic evolution of some metamorphic belts]. *MTA Enstitüsü Dergisi*, **83**, 178–184 [in Turkish].
- Boynnton, W. V. 1984. Cosmochemistry of the rare earth elements: meteorite studies. In *Rare Earth Elements* (Henderson, P., ed.), pp. 63–114. Elsevier, Amsterdam.
- Boztug, D. 1998. Post-collisional central Anatolian alkaline plutonism, Turkey. *Turkish Journal of Earth Sciences*, **7**(3), 145–165.
- Boztug, D. 2000. S-I-A-type intrusive associations: geodynamic significance of synchronism between metamorphism and magmatism in Central Anatolia, Turkey. In *Tectonics and Magmatism in Turkey and the Surrounding Area* (Bozkurt, E., Winchester, J. A. & Piper, J. D. A., eds), *Geological Society of London, Special Publications*, **73**, 441–458.
- Boztug, D., Arehart, G. B., Platevoet, B., Harlavan, Y. & Bonin, B. 2007. High-K, calc-alkaline I-type granitoids from the composite Yozgat batholith generated in a post-collisional setting following continent-oceanic island arc collision in central Anatolia, Turkey. *Mineralogy and Petrology*, **91**(3–4), 191–223.
- Bussy, F. 1991. Enclaves of the Late Miocene Monte Capanne granite, Elba Island, Italy. In *Enclaves and Granite Petrology* (Didier, J. & Barbarin, B., eds), pp. 167–178. Elsevier.
- Cantagrel, J. M., Didier, J. & Gourgaud, A. 1984. Magma mixing – origin of intermediate rocks and enclaves from volcanism to plutonism. *Physics of the Earth and Planetary Interiors*, **35**(1–3), 63–76.
- Çevikbaş, A., Boztug, D., Demirkol, C., Yılmaz, S., Akyıldız, M., Açlan, M., Demir, Ö. & Taş, R. 1995. Horoz plütununun (Ulukışla-Niğde) oluşumunda dengelenmiş hibrid sistemin mineralojik ve jeokimyasal kanıtları [Mineralogical and geochemical evidences of the equilibrated hybrid system in the formation of the Horoz (Ulukışla-Niğde) pluton]. *Geological Bulletin of Turkey*, **10**, 62–67 [in Turkish].
- Chappell, B. W. 1996. Magma mixing and the production of compositional variation within granite suites: evidence from the granites of southeastern Australia. *Journal of Petrology*, **37**(3), 449–470.
- Chappell, B. W. & White, A. J. R. 1992. I- and S-type granites in the Lachlan Fold Belt. *Transactions of the Royal Society of Edinburgh, Earth and Environmental Science*, **83**(1–2), 1–26.
- Chappell, B. W., White, A. J. R. & Wyborn, D. 1987. The importance of residual source material (restite) in granite petrogenesis. *Journal of Petrology*, **28**(6), 1111–1138.
- Chen, B., Chen, Z. C. & Jahn, B. M. 2009. Origin of mafic enclaves from the Taihang Mesozoic orogen, north China craton. *Lithos*, **110**(1–4), 343–358.
- Chen, Y. D., Price, R. C. & White, A. J. R. 1989. Inclusions in three S-type granites from Southeastern Australia. *Journal of Petrology*, **30**(5), 1181–1218.
- Clark, M. & Robertson, A. 2002. The role of the Early Tertiary Ulukışla Basin, Southern Turkey, in suturing of the Mesozoic Tethys Ocean. *Journal of the Geological Society, London*, **159**, 673–690.
- Clemens, J. D. & Wall, V. J. 1988. Controls on the mineralogy of S-type volcanic and plutonic rocks. *Lithos*, **21**(1), 53–66.
- Condie, K. C. 2005. TTGs and adakites: are they both slab melts? *Lithos*, **80**(1–4), 33–44.
- Dahlquist, J. A. 2002. Mafic microgranular enclaves: early segregation from metaluminous magma (Sierra de Chepes), Pampean Ranges, NW Argentina. *Journal of South American Earth Sciences*, **15**(6), 643–655.
- Davidson, J., MacPherson, C. & Turner, S. 2007a. Amphibole control in the differentiation of arc magmas. *Geochimica et Cosmochimica Acta*, **71**(15), A204.
- Davidson, J., Turner, S., Handley, H., Macpherson, C. & Dosseto, A. 2007b. Amphibole “sponge” in arc crust? *Geology*, **35**(9), 787–790.
- Davidson, J. P., Turner, S. P. & Macpherson, C. G. 2008. Water storage and amphibole control in arc magma differentiation. *Geochimica et Cosmochimica Acta*, **72**(12), A201.
- Debon, F. 1991. Comparative major element chemistry in various “microgranular enclave-plutonic host” pairs. In *Enclaves and Granite Petrology* (Didier, J. & Barbarin, B., eds), pp. 293–312. Elsevier, Amsterdam.
- Debon, F. & Le Fort, P. 1983. A chemical–mineralogical classification of common plutonic rocks and associations. *Transactions of the Royal Society of Edinburgh, Earth and Environmental Sciences*, **73**(03), 135–149.
- Didier, J. 1973. *Granites and Their Enclaves. The Bearing of Enclaves on the Origin of Granites. Developments in Petrology 3*. Elsevier Scientific Publishing Co., Amsterdam, xiv + 393 pp.

- Didier, J. & Barbarin, B. 1991. *Enclaves and Granite Petrology*. Elsevier, Amsterdam, 625 pp.
- Didier, J., Duthou, J. L. & Lameyre, J. 1982. Mantle and crustal granites: genetic classification of orogenic granites and the nature of their enclaves. *Journal of Volcanology and Geothermal Research*, **14**(1–2), 125–132.
- Dilek, Y., Garver, J. I. & Whitney, D. L. 1997. Extensional exhumation, uplift, and crustal cooling in a collision orogen and the geomorphic response, central Anatolia – Turkey. *Geological Society of America Abstracts with Programs*, **29**, A474.
- Dilek, Y., Thy, P., Hacker, B. & Grundvig, S. 1999. Structure and petrology of Tauride ophiolites and mafic dike intrusions (Turkey): implications for the Neotethyan ocean. *Geological Society of America Bulletin*, **111**(8), 1192–1216.
- Dodge, F. C. W. & Kistler, R. W. 1990. Some additional observations on inclusions in the granitic rocks of the Sierra Nevada. *Journal of Geophysical Research*, **95**(B11), 17841–17848.
- Donaire, T., Pascual, E., Pin, C. & Duthou, J. L. 2005. Microgranular enclaves as evidence of rapid cooling in granitoid rocks: the case of the Los Pedroches granodiorite, Iberian Massif, Spain. *Contributions to Mineralogy and Petrology*, **149**(3), 247–265.
- Donnelly, T. W. & Rogers, J. J. W. 1980. Igneous series in island arc: the northeastern Caribbean compared with worldwide island-arc assemblages. *Bulletin of Volcanology*, **43**(2), 347–382.
- Dorais, M. J., Whitney, J. A. & Roden, M. F. 1990. Origin of mafic enclaves in the Dinkey Creek Pluton Central Sierra Nevada Batholith, California. *Journal of Petrology*, **31**(4), 853–881.
- Drummond, M. S. & Defant, M. J. 1990. A model for Trondhjemite-Tonalite-Dacite genesis and crustal growth via slab melting: Archean to modern comparisons. *Journal of Geophysical Research: Solid Earth*, **95**(B13), 21503–21521.
- Feeley, T. C., Wilson, L. F. & Underwood, S. J. 2008. Distribution and compositions of magmatic inclusions in the Mount Helen dome, Lassen Volcanic Center, California: insights into magma chamber processes. *Lithos*, **106**(1–2), 173–189.
- Ferré, E. C. & Leake, B. E. 2001. Geodynamic significance of early orogenic high-K crustal and mantle melts: example of the Corsica Batholith. *Lithos*, **59**(1–2), 47–67.
- Foley, S., Tiepolo, M. & Vannucci, R. 2002. Growth of early continental crust controlled by melting of amphibolite in subduction zones. *Nature*, **417**, 837–840.
- Fourcade, S. & Javoy, M. 1991. Sr–Nd–O isotopic features of mafic microgranular enclaves and host granitoids from the Pyrenees, France: evidence for their hybrid nature and inference on their origin. In *Enclaves and Granite Petrology* (Didier, J. & Barbarin, B., eds), pp. 345–366. Elsevier, Amsterdam.
- Frost, T. P. & Mahood, G. A. 1987. Field, chemical, and physical constraints on mafic–felsic magma interaction in the Lamarck Granodiorite, Sierra Nevada, California. *Geological Society of America Bulletin*, **99**, 272–291.
- Geist, D., Howard, K. A. & Larson, P. 1995. The generation of oceanic rhyolites by crystal fractionation: the basalt-rhyolite association at Volcán Alcedo, Galápagos Archipelago. *Journal of Petrology*, **36**(4), 965–982.
- Goncuoglu, M. C., Toprak, V., Kuscü, U., Erler, A. & Olgun, E. 1991. *Geology of the Western Part of the Central Anatolian Massif, Part 1: Southern Section*. Unpublished Report No. 2909, Turkish Petroleum Company Project [in Turkish].
- Gorur, N., Oktay, F., Seymen, I. & Sengor, A. M. C. 1984. Paleotectonic evolution of the Tuzgolu basin complex, central Turkey: sedimentary record of a Neo-Tethyan closure. In *The Geological Evolution of the Eastern Mediterranean* (Dixon, J. E. & Robertson, A. H. F., eds), *Geological Society of London, Special Publication*, **17**, 455–466.
- Gorur, N., Tuysuz, O. & Sengor, A. M. C. 1998. Tectonic evolution of the central Anatolian basins. *International Geology Review*, **40**(9), 831–850.
- Green, T. H. 1995. Significance of Nb/Ta as an indicator of geochemical processes in the crust-mantle system. *Chemical Geology*, **120**(3–4), 347–359.
- Harris, N. B. W., Pearce, J. A. & Tindle, A. G. 1986. Geochemical characteristics of collision zone magmatism. In *Collision Tectonics* (Coward, M. P. & Reis, A. C., eds), *Geological Society of London, Special Publication*, **19**, 67–81.
- Hart, S. R. 1984. A large-scale isotope anomaly in the Southern Hemisphere mantle. *Nature*, **309**(5971), 753–757.
- Hawkesworth, C. J. & Kemp, A. I. S. 2006. Using hafnium and oxygen isotopes in zircons to unravel the record of crustal evolution. *Chemical Geology*, **226**(3–4), 144–162.
- He, Z.-Y., Xu, X.-S. & Niu, Y. 2010. Petrogenesis and tectonic significance of a Mesozoic granite–syenite–gabbro association from inland South China. *Lithos*, **119**(3–4), 621–641.
- Helz, R. T. 1976. Phase relations of basalts in their melting ranges at $\text{PH}_2\text{O} = 5$ kb. Part II. Melt composition. *Journal of Petrology*, **17**(2), 139–193.
- Hochstaedter, A. G., Gill, J. B. & Morris, J. D. 1990. Volcanism in the Sumisu Rift, II. Subduction and non-subduction related components. *Earth and Planetary Science Letters*, **100**(1–3), 195–209.
- Hoffmann, J. E., Münker, C., Næraa, T., Rosing, M. T., Herwartz, D., Garbe-Schönberg, D. & Svahnberg, H. 2011. Mechanisms of Archean crust formation by high precision HFSE systematics on TTGs. *Geochimica et Cosmochimica Acta*, **75**(15), 4157–4178.
- Huang, X.-L., Xu, Y.-G., Lan, J.-B., Yang, Q.-J. & Luo, Z.-Y. 2009. Neoproterozoic adakitic rocks from Mopanshan in the western Yangtze Craton: partial melts of a thickened lower crust. *Lithos*, **112**(3–4), 367–381.
- Icenhower, J. & London, D. 1996. Experimental partitioning of Rb, Cs, Sr, and Ba between alkali feldspar and peraluminous melt. *American Mineralogist*, **81**(5–6), 719–734.
- İlbeyli, N., Pearce, J. A., Thirlwall, M. F. & Mitchell, J. G. 2004. Petrogenesis of collision-related plutonics in Central Anatolia, Turkey. *Lithos*, **72**(3–4), 163–182.
- Isik, F. & Kocak, K. 2005. Petrographical and geochemical characteristics of Ekecekdagi granitoid (Northeast of Aksaray). *Geosound*, **46**, 83–105.
- Johnston, A. D. & Wyllie, P. J. 1988. Interaction of granitic and basic magmas: experimental observations on contamination processes at 10 kbar with H_2O . *Contributions to Mineralogy and Petrology*, **98**(3), 352–362.

- Kadioglu, Y. K. & Dilek, Y. 2010. Structure and geochemistry of the adakitic Horoz granitoid, Bolkar Mountains, south-central Turkey, and its tectonomagmatic evolution. *International Geology Review*, **52**(4–6), 505–535.
- Kadioglu, Y. K. & Güleç, N. 1996. Structural setting of gabbros in the Agaçören granitoid: implications from geological and geophysical (resistivity) data. *TÜBITAK Turkish Journal of Earth Sciences*, **5**, 153–159 [in Turkish, with English abstract].
- Kadioglu, Y. K., Dilek, Y., Gulec, N. & Foland, K. A. 2003. Tectonomagmatic evolution of bimodal plutons in the Central Anatolian Crystalline Complex, Turkey. *The Journal of Geology*, **111**(6), 671–690.
- Kadioglu, Y. K., Dilek, Y. & Foland, K. A. 2006. Slab break-off and syncollisional origin of the Late Cretaceous magmatism in the Central Anatolian crystalline complex, Turkey. *Geological Society of America, Special Paper*, **409**, 381–415.
- Kamber, B. S., Ewart, A., Collerson, K. D., Bruce, M. C. & McDonald, G. D. 2002. Fluid-mobile trace element constraints on the role of slab melting and implications for Archean crustal growth models. *Contributions to Mineralogy and Petrology*, **144**(1), 38–56.
- Kaygusuz, A. & Aydınçakır, E. 2009. Mineralogy, whole-rock and Sr–Nd isotope geochemistry of mafic microgranular enclaves in Cretaceous Dagbasi granitoids, Eastern Pontides, NE Turkey: evidence of magma mixing, mingling and chemical equilibration. *Chemie der Erde – Geochemistry*, **69**(3), 247–277.
- Kaynak, M. & Akcakaya, M. 2006. *The Project of the Aeromagnetic Map of Turkey*. MTA report No. 10794.
- Kemp, A. I. S. & Hawkesworth, C. J. 2003. Granitic perspectives on the generation and secular evolution of the continental crust. In *Treatise on Geochemistry, Vol 3* (Rudnick, R. L., ed.), pp. 349–410. Elsevier, Oxford, UK.
- Kemp, A. I. S., Hawkesworth, C. J., Foster, G. L., Paterson, B. A., Woodhead, J. D., Hergt, J. M., Gray, C. M. & Whitehouse, M. J. 2007. Magmatic and crustal differentiation history of granitic rocks from Hf–O isotopes in zircon. *Science*, **315**(5814), 980–983.
- Klein, M., Stosch, H. G. & Seck, H. A. 1997. Partitioning of high field-strength and rare-earth elements between amphibole and quartz-dioritic to tonalitic melts: an experimental study. *Chemical Geology*, **138**(3–4), 257–271.
- Klein, M., Stosch, H. G., Seck, H. A. & Shimizu, N. 2000. Experimental partitioning of high field strength and rare earth elements between clinopyroxene and garnet in andesitic to tonalitic systems. *Geochimica et Cosmochimica Acta*, **64**(1), 99–115.
- Kocak, K. 1993. *The Petrology and Geochemistry of the Ortaköy Area, Central Turkey*. PhD Thesis, Glasgow University.
- Kocak, K. 2006. Hybridization of mafic microgranular enclaves: mineral and whole-rock chemistry evidence from the Karamadazi Granitoid, Central Turkey. *International Journal of Earth Sciences*, **95**(4), 587–607.
- Kocak, K. 2008. Mineralogy, geochemistry, and Sr–Nd isotopes of the Cretaceous leucogranite from Karamadaz (Kayseri), central Turkey: implications for their sources and geological setting. *Canadian Journal of Earth Sciences*, **45**(8), 949–968.
- Kocak, K. & Leake, B. E. 1994. The petrology of the Ortaköy district and its ophiolite at the western edge of the Middle Anatolian Massif, Turkey. *Journal of African Earth Sciences*, **18**(2), 163–174.
- Kocak, K., Zedef, V. & Kansun, G. 2011. Magma mixing/mingling in the Eocene Horoz (Nigde) granitoids, Central southern Turkey: evidence from mafic microgranular enclaves. *Mineralogy and Petrology*, **103**(1–4), 149–167.
- Kuscu, G. G., Kuşcu, R. M., Tosdal, T. D. & Ulrich, R. F. 2010. Magmatism in the southeastern Anatolian orogenic belt: transition from arc to post-collisional setting in an evolving orogeny. In *Sedimentary Basin Tectonics from the Black Sea and Caucasus to the Arabian Platform* (Sosson, M., Kaymakci, N., Stephenson, R. A., Bergerat, F. & Starostenko, V., eds), *Geological Society of London, Special Publications*, **340**, 437–460.
- Langmuir, C., Vocke, R., Hanson, G. & Hart, S. 1978. A general mixing equation with applications to Icelandic basalts. *Earth and Planetary Science Letters*, **37**(3), 380–392.
- Leshner, C. E. 1990. Decoupling of chemical and isotopic exchange during magma mixing. *Nature*, **344**(6263), 235–237.
- Li, W.-X., Li, X.-H. & Li, Z.-X. 2005. Neoproterozoic bimodal magmatism in the Cathaysia Block of South China and its tectonic significance. *Precambrian Research*, **136**(1), 51–66.
- Li, X. H., Li, W. X., Wang, X. C., Li, Q. L., Liu, Y. & Tang, G. Q. 2009. Role of mantle-derived magma in genesis of early Yanshanian granites in the Nanling Range, South China: in situ zircon Hf–O isotopic constraints. *Science in China Series D–Earth Sciences*, **52**(9), 1262–1278.
- Liu, J. F., Chi, X. G., Zhao, Z., Hu, Z. C. & Chen, J. Q. 2013. Zircon U–Pb age and petrogenetic discussion on Jianshetun adakite in Balinyouqi, Inner Mongolia. *Acta Petrologica Sinica*, **29**(3), 827–839.
- López-Ruiz, J. & Cebriá, J. M. 1990. *Geoquímica de los Procesos Magmáticos*. Rueda, Madrid, 168 pp.
- Martin, H. 1986. Effect of steeper Archean geothermal gradient on geochemistry of subduction-zone magmas. *Geology*, **14**(9), 753–756.
- Martin, H. 1999. Adakitic magmas: modern analogues of Archean granitoids. *Lithos*, **46**(3), 411–429.
- Martin, H. & Moyen, J. F. 2002. Secular changes in tonalite–trondhjemite–granodiorite composition as markers of the progressive cooling of Earth. *Geology*, **30**(4), 319–322.
- Martin, H., Smithies, R. H., Rapp, R., Moyen, J. F. & Champion, D. 2005. An overview of adakite, tonalite–trondhjemite–granodiorite (TTG), and sanukitoid: relationships and some implications for crustal evolution. *Lithos*, **79**(1–2), 1–24.
- Matsui, Y., Onuma, N., Nagasawa, H., Higuchi, H. & Banno, S. 1977. Crystal structure control in trace element partition between crystal and magma. *Tectonics*, **100**, 315–324.
- McCulloch, M. T. & Gamble, J. A. 1991. Geochemical and geodynamical constraints on subduction zone magmatism. *Earth and Planetary Science Letters*, **102**(3–4), 358–374.
- Noyes, H. J., Frey, F. A. & Wones, D. R. 1983. A tale of two plutons: geochemical evidence bearing on the origin and differentiation of the Red Lake and Eagle Peak Plutons, Central Sierra Nevada, California. *The Journal of Geology*, **91**(5), 487–509.
- Oberc-Dziedzic, T., Pin, C. & Kryza, R. 2005. Early Palaeozoic crustal melting in an extensional setting: petrological and Sm–Nd evidence from the Izera granite-gneisses, Polish

- Sudetes. *International Journal of Earth Sciences*, **94**(3), 354–368.
- Orsini, J. B., Cocirta, C. & Zorpi, M. J. 1991. Genesis of mafic microgranular enclaves through differentiation of basic magmas, mingling and chemical exchanges with their host granitoid magmas. In *Enclaves and Granite Petrology, Vol. 13* (Didier, J. & Barbarin, B., eds), pp. 445–464. Elsevier, Amsterdam.
- Ozer, E., Koc, H. & Ozsayar, T. Y. 2004. Stratigraphical evidence for the depression of the northern margin of the Menderes-Tauride Block (Turkey) during the Late Cretaceous. *Journal of Asian Earth Sciences*, **22**(5), 401–412.
- Parlak, O., Colakoglu, A., Donmez, C., Sayak, H., Yildirim, N., Turkel, A. & Odabasi, I. 2013a. Geochemistry and tectonic significance of ophiolites along the Izmir-Ankara-Erzincan Suture Zone in northeastern Anatolia. In *Geological Development of Anatolia and the Easternmost Mediterranean Region* (Robertson, A. H. F., Parlak, O. & Ünlügenç, U. C., eds), *Geological Society of London, Special Publications*, **372**(1), 75–105.
- Parlak, O., Karaoğlan, F., Rızaoğlu, T., Klötzli, U., Koller, F. & Billor, Z. 2013b. U–Pb and ^{40}Ar – ^{39}Ar geochronology of the ophiolites and granitoids from the Tauride belt: implications for the evolution of the Inner Tauride suture. *Journal Geodynamics*, **65**, 22–37.
- Pearce, J. 1996. Sources and settings of granitic rocks. *Episodes*, **19**(4), 120–125.
- Pearce, J. A., Harris, N. B. W. & Tindle, A. G. 1984. Trace element discrimination diagrams for the tectonic interpretation of granitic rocks. *Journal of Petrology*, **25**(4), 956–983.
- Peccerillo, A. & Taylor, S. R. 1976. Geochemistry of Eocene calc-alkaline volcanic rocks of the Kastamonu area, northern Turkey. *Contributions to Mineralogy and Petrology*, **58**(1), 63–81.
- Pe-Piper, G., Piper, D. J. W. & Matarangas, D. 2002. Regional implications of geochemistry and style of emplacement of Miocene I-type diorite and granite, Delos, Cyclades, Greece. *Lithos*, **60**(1–2), 47–66.
- Petford, N. & Atherton, M. 1996. Na-rich partial melts from newly underplated basaltic crust: the Cordillera Blanca Batholith, Peru. *Journal of Petrology*, **37**(6), 1491–1521.
- Philpotts, J. A. & Schnetzler, C. C. 1970. Phenocryst-matrix partition coefficients for K, Rb, Sr and Ba, with applications to anorthosite and basalt genesis. *Geochimica et Cosmochimica Acta*, **34**(3), 307–322.
- Pin, C., Binon, M., Belin, J. M., Barbarin, B. & Clemens, J. D. 1990. Origin of microgranular enclaves in granitoids: equivocal Sr–Nd evidence from Hercynian rocks in the Massif Central (France). *Journal of Geophysical Research: Solid Earth*, **95**(B11), 17821–17828.
- Poli, G. & Tommasini, S. 1991. Model for the origin and significance of Microgranular enclaves in calc-alkaline granitoids. *Journal of Petrology*, **32**(3), 657–666.
- Qian, Q. & Wang, Y. 1999. Geochemical characteristics of bimodal volcanic suites from different tectonic settings. *Geology and Geochemistry*, **27**, 29–32.
- Rapp, R. P. & Watson, E. B. 1995. Dehydration melting of metabasalt at 8–32 kbar: implications for continental growth and crust-mantle recycling. *Journal of Petrology*, **36**(4), 891–931.
- Rapp, R. P., Watson, E. B. & Miller, C. F. 1991. Partial melting of amphibolite eclogite and the origin of Archean trondhjemites and tonalites. *Precambrian Research*, **51**(1–4), 1–25.
- Rapp, R. P., Shimizu, N., Norman, M. D. & Applegate, G. S. 1999. Reaction between slab-derived melts and peridotite in the mantle wedge: experimental constraints at 3.8 GPa. *Chemical Geology*, **160**(4), 335–356.
- Rudnick, R. L. & Fountain, D. M. 1995. Nature and composition of the continental crust – a lower crustal perspective. *Reviews of Geophysics*, **33**(3), 267–309.
- Sen, C. & Dunn, T. 1994. Dehydration melting of a basaltic composition amphibolite at 1.5 and 2.0 GPa – implications for the origin of adakites. *Contributions to Mineralogy and Petrology*, **117**(4), 394–409.
- Shand, S. J. 1943. *Eruptive Rocks; Their Genesis, Composition, Classification, and their Relation to Ore Deposits, with a Chapter on Meteorites*. Hafner Publishing Co., New York, 488 pp.
- Shellnutt, J. G., Jahn, B. M. & Dostal, J. 2010. Elemental and Sr–Nd isotope geochemistry of microgranular enclaves from peralkaline A-type granitic plutons of the Emeishan large igneous province, SW China. *Lithos*, **119**(1–2), 34–46.
- Shu, L. S., Zuhu, W. B., Wang, B., Faure, M., Charvet, J. & Cluzel, D. 2005. The post-collision intracontinental rifting and olistostrome on the southern slope of Bogda Mountains, Xinjiang. *Acta Petrologica Sinica*, **21**(1), 25–36.
- Silva, M. M. V. G., Neiva, A. M. R. & Whitehouse, M. J. 2000. Geochemistry of enclaves and host granites from the Nelas area, central Portugal. *Lithos*, **50**(1–3), 153–170.
- Smithies, R. H. 2000. The Archean tonalite–trondhjemite–granodiorite (TTG) series is not an analogue of cenozoic adakite. *Earth and Planetary Science Letters*, **182**(1), 115–125.
- Smithies, R. H. & Champion, D. C. 2000. The Archean high-Mg diorite suite: links to tonalite–trondhjemite–granodiorite magmatism and implications for early Archean crustal growth. *Journal of Petrology*, **41**(12), 1653–1671.
- Smithies, R. H., Champion, D. C. & Cassidy, K. F. 2003. Formation of Earth’s early Archean continental crust. *Precambrian Research*, **127**(1–3), 89–101.
- Smithies, R. H., Champion, D. C. & Van Kranendonk, M. J. 2009. Formation of Paleoproterozoic continental crust through infracrustal melting of enriched basalt. *Earth and Planetary Science Letters*, **281**(3–4), 298–306.
- Springer, W. & Seck, H. A. 1997. Partial fusion of basic granulites at 5 to 15 kbar: implications for the origin of TTG magmas. *Contributions to Mineralogy and Petrology*, **127**(1–2), 30–45.
- Spulber, S. D. & Rutherford, M. J. 1983. The origin of rhyolite and plagiogranite in oceanic crust: an experimental study. *Journal of Petrology*, **24**(1), 1–25.
- Srogi, L. & Lutz, T. 1990. Three-dimensional morphologies of metasedimentary and mafic enclaves from Ascutney Mountain, Vermont. *Journal of Geophysical Research*, **95**(B11), 17829–17840.
- Sun, S.-S. 1980. Lead isotopic study of young volcanic rocks from mid-ocean ridges, ocean islands and island arcs. *Philosophical Transactions of the Royal Society of*

- London A: *Mathematical, Physical and Engineering Sciences*, **297**(1431), 409–445.
- Sun, S. S. & McDonough, W. F. 1989. Chemical and isotopic systematics of oceanic basalts: implications for mantle composition and processes. In *Magmatism in the Ocean Basins* (Saunders, A. D. & Norry, M. J., eds), *Geological Society of London, Special Publications*, **42**, 313–345.
- Taylor, S. R. & McLennan, S. M. 1985. *The Continental Crust, its Composition and Evolution: an Examination of the Geochemical Record preserved in Sedimentary Rocks*. Blackwell Scientific Publications, Oxford, 312 pp.
- Taylor, S. R. & McLennan, S. M. 1995. The geochemical evolution of the continental crust. *Reviews of Geophysics*, **33**(2), 241–265.
- Tepper, J. H., Nelson, B. K., Bergantz, G. W. & Irving, A. J. 1993. Petrology of the Chilliwack batholith, North Cascades, Washington: generation of calc-alkaline granitoids by melting of mafic lower crust with variable water fugacity. *Contributions to Mineralogy and Petrology*, **113**(3), 333–351.
- Todt, W., Cliff, R. A., Hanser, A. & Hofmann, A. W. 1996. Evaluation of a ^{202}Pb – ^{205}Pb double spike for high precision lead isotope analyses, In *Earth Processes: Reading the Isotope Code* (Basu, A. & Hart, S., eds), *American Geophysical Union, Geophysical Monograph Series*, **95**, 429–437.
- Tulloch, A. J. & Challis, G. A. 2000. Emplacement depths of Paleozoic–Mesozoic plutons from western New Zealand estimated by hornblende–Al geobarometry. *New Zealand Journal of Geology and Geophysics*, **43**(4), 555–567.
- Vernon, R. H. 1984. Microgranitoid enclaves in granites globules of hybrid magma quenched in a plutonic environment. *Nature*, **309**(5967), 438–439.
- Vernon, R. H. 1990. Crystallization and hybridism in microgranitoid enclave magmas: microstructural evidence. *Journal of Geophysical Research*, **95**(B11), 17849–17859.
- Vorontsov, A. A., Yarmolyuk, V. V. & Baikin, D. N. 2004. Structure and composition of the Early Mesozoic volcanic series of the Tsagan–Khurtei Graben, western Transbaikalia: geological, geochemical, and isotopic data. *Geochemistry International*, **42**(11), 1046–1061.
- Waight, T. E., Wiebe, R. A., Krogstad, E. J. & Walker, R. J. 2001. Isotopic responses to basaltic injections into silicic magma chambers: a whole-rock and microsampling study of macrorhythmic units in the Pleasant Bay layered gabbro-diorite complex, Maine, USA. *Contributions to Mineralogy and Petrology*, **142**(3), 323–335.
- Wang, Q., Xu, J. F., Jian, P., Bao, Z. W., Zhao, Z. H., Li, C. F., Xiong, X. L. & Ma, J. L. 2006. Petrogenesis of adakitic porphyries in an extensional tectonic setting, dexing, South China: implications for the genesis of porphyry copper mineralization. *Journal of Petrology*, **47**(1), 119–144.
- West, D. P., Coish, R. A. & Tomascak, P. B. 2004. Tectonic setting and regional correlation of Ordovician meta-volcanic rocks of the Casco Bay Group, Maine: evidence from trace element and isotope geochemistry. *Geological Magazine*, **141**(02), 125–140.
- White, A. J. R., Chappell, B. W. & Wyborn, D. 1999. Application of the restite model to the Deddick Granodiorite and its enclaves – a reinterpretation of the observations and data of Maas et al. (1997). *Journal of Petrology*, **40**(3), 413–421.
- Whitney, D., Lefebvre, C., Thomson, S. N. & Teyssier, C. P. 2015. Uplift and exhumation in central Anatolia: new results from low-temperature chronometry in a deeply incised granite in the Central Tauride Mountains, Turkey. In *AGU Fall Meeting, San Francisco, 14–18 December; Mantle, Crust, and Surface Dynamics in the Mediterranean System I Posters*.
- Wiebe, R. A., Smith, D., Sturm, M., King, E. M. & Seckler, M. S. 1997. Enclaves in the Cadillac Mountain granite (coastal Maine): samples of hybrid magma from the base of the chamber. *Journal of Petrology*, **38**(3), 393–423.
- Wilson, M. 1989. *Igneous Petrogenesis. A Global Tectonic Approach*. Unwin Hyman, London, 466 pp.
- Winther, K. T. & Newton, R. C. 1991. Experimental melting of hydrous low-K tholeiite: evidence on the origin of Archean craton. *Bulletin of the Geological Society of Denmark*, **39**(2), 213–228.
- Wolf, M. B. & Wyllie, P. J. 1994. Dehydration-melting of solid amphibolite at 10 kbar: textural development, liquid interconnectivity and applications to the segregation of magmas. *Contributions to Mineralogy and Petrology*, **44**(3), 151–179.
- Zamora, D. 2000. *Fusion de la croûte océanique subductée: approche expérimentale et géochimique*. Université Thesis, Université Blaise Pascal, Clermont-Ferrand, 314 pp.
- Zhu, J. C., Wang, R. C. & Xie, L. 2009. Magma mingling origin of mafic microgranular enclaves in Guposhan granite pluton, South China. *Geochimica et Cosmochimica Acta*, **73**(13), A1531.

Litosfäärilise vahevöö ja maakoorettekkega magmade suhted Horozi intrusiooni (Türgi) tekkes kivimi geokeemiliste ning Sr-Nd-Pb isotoopgeoloogiliste andmete alusel

Kerim Kocak ja Veysel Zedef

Horozi intrusioon on üles ehitatud graniitsetest ja granodioriidsetest kivimitest, milles on rohkesti mikrogranulaarseid suletisi. Keemiliselt on intrusiooni kivimid lubileeliselised kuni šooniitised (rikastunud Rb ja K ning vaesestunud Y ja Lu osas). Graniitne ja granodioriidne kivim on geokeemiliselt sarnane tonaliitse-trondheimiitse assotsiatsiooni kivimile (TTG), viidates võimalikule magmatektele paksenenud alumise maakoore ülessulamisel. Nii intrusiooni kivim kui ka selles olevad mikrogranulaarsed suletised näitavad madalaid $^{87}\text{Sr}/^{86}\text{Sr}$ suhteid (vastavalt 0,7046–0,7051 ja 0,7047–0,7058), madalaid epsiloni Nd väärtusi (–1,8–0,7) ning väga radiogeenset $^{208}\text{Pb}/^{204}\text{Pb}$ suhet (39,43–39,47 ja 39,39–39,54). Kivimite elemendiline ja isotoopgeokeemiline andmestik viitab intrusiooni tekkele läbi litosfäärilise vahevöö ning maakoorettekkeliste magmade segunemise.